INVESTIGATION OF MACHINABILITY OF GG25 GRAY CAST IRON

A THESIS SUBMITTED TO
THE GRADUATE SCHOOL OF NATURAL AND APPLIED SCIENCES OF
UNIVERSITY OF THE TURKISH AERONAUTICAL ASSOCIATION

BY

SAMET EMRE BİLİM

IN PARTIAL FULFILLMENT OF THE
REQUIREMENTS FOR
THE DEGREE OF MASTER
IN
MECHANICAL AND AERONAUTICAL ENGINEERING

AUGUST 2023

INVESTIGATION OF MACHINABILITY OF GG25 GRAY CAST IRON

A THESIS SUBMITTED TO
THE GRADUATE SCHOOL OF NATURAL AND APPLIED SCIENCES OF
UNIVERSITY OF THE TURKISH AERONAUTICAL ASSOCIATION

BY

SAMET EMRE BİLİM

IN PARTIAL FULFILLMENT OF THE
REQUIREMENTS FOR
THE DEGREE OF MASTER
IN
MECHANICAL AND AERONAUTICAL ENGINEERING

Assoc. Prof. Dr. Suat Dengiz

AUGUST 2023

Approval of the thesis:

INVESTIGATION OF MACHINABILITY OF GG25 GRAY CAST IRON

submitted by **SAMET EMRE BİLİM** in fulfillment of the requirements for the degree of **Master in Mechanical and Aeronautical Engineering, University of Turkish Aeronautical Association** by,

Assoc. Prof. Dr. Suat Dengiz
Dean, Graduate School of **Natural and Applied Sciences** _____

Assoc. Prof. Dr. Muhammed ARAS
Co-Supervisor, **Department of Mechanical Engineering**, **Başkent University** _____

Examining Committee Members:

Assoc. Prof. Dr. Suat Dengiz
Mechanical Engineering, UTAA _____

Assoc. Prof. Dr. Emine Deniz Tekin
Computer Engineering, UTAA _____

Assoc. Prof. Dr. Erdem Çiftçi
Energy Systems Engineering, Gazi University _____

Date: 01.08.2023

I hereby declare that all information in this document has been obtained and presented in accordance with academic rules and ethical conduct. I also declare that, as required by these rules and conduct, I have fully cited and referenced all material and results that are not original to this work.

Name, Surname: Samet Emre, Bilim

Signature :

ABSTRACT

INVESTIGATION OF MACHINABILITY OF GG25 GRAY CAST IRON

Bilim, Samet Emre

Degree of Master in Mechanical and Aeronautical Engineering,

Supervisor: Assoc. Prof. Dr. Suat DENGİZ

Co-Supervisor: Assoc. Prof. Dr. Muhammed ARAS

August 2023, 74 Pages

Bu deneysel çalışmada CNC Frezeleme işleminde GG25 gri dökme demirin karbür uçlarla işlenebilirliği araştırılmıştır. Kesme parametreleri ilerleme hızı, kesme derinliği ve kesme hızı olarak seçilirken, çıkış parametreleri yüzey pürüzlülüğü, kesme kuvveti ve güç tüketimi olarak seçildi. Deneyin tasarımı için Taguchi L27 tam faktöriyel kullanılmıştır. Toplam 27 deney yapılmış ve sonuçları analiz etmek için yanıt yüzey metodolojisi (RSM) ve varyans analizi (ANOVA) kullanılmıştır. Ayrıca, araştırma çıktılarını daha verimli hale getirmek için CNC freze makinesinden talaşları çıkarmadan optimum koşullarda çalışmak üzere bilyalı çubuk testleri yapılmıştır. Ek olarak, deneysel sonuçlara yaklaşmak için ANSYS dinamik analizi kullanılmıştır. Bu çalışmanın sonuçları, ilerleme hızının ardından kesme derinliğinin çıktı parametreleri üzerinde en önemli etkiye sahip olduğunu göstermiştir. Deneysel verilere göre, besleme hızı arttıkça yüzey pürüzlülüğü artarken, tüm giriş parametrelerinin seviyesi

arttıkça güç tüketimi ve kesme kuvveti de artar. Yüzey pürüzlülüğü belirleme katsayısı %96,58'dir. Bununla birlikte, kesme kuvveti ve güç tüketimi sırasıyla% 97.65 ve% 91.78 doğrulukla modellenmiştir. İlerleme oranı, %82,37 ile yüzey pürüzlülüğü üzerinde en etkili faktördür. Kesme derinliği, sırasıyla %68,82 ve %49,34 ile hem kesme kuvveti hem de güç tüketimi için en önemli faktördür. Yüzey pürüzlülüğü için hata yüzdesi% 3.42, kesme kuvveti için% 2.35 ve sonuçlardan% 8.22'dir. Son olarak, altı rastgele deney için doğrulama testi yapıldı ve sonuçlar, GG25 gri dökme demir için geliştirilen regresyon denklemlerinden tahmin edilen sonuçla karşılaştırıldı. Sonuç olarak, GG 25 gri dökme demirin işlenmesi için optimum kesme parametreleri şu şekilde belirlenmiştir: Vc: 300 m/dak, f: 2000 mm/dak ve ap: 0,1 mm.

Keywords: GG25 Gray Cast Iron, Carbide Insert, Surface Roughness, Cutting Force, Power Consumption, Response Surface Methodology, ANOVA.

ÖZ

GG25 GRİ DÖKÜM DEMİRİN İŞLENEBİLİRLİĞİNİN İNCELENMESİ

Bilim, Samet Emre

Makine ve Uçak Mühendisliği Yüksek Lisans Derecesi,

Danışman: Doç. Dr. Suat DENGİZ

Eş Danışman: Doç. Dr. Muhammed ARAS

Ağustos 2023, 74 Sayfa

Bu deneysel çalışmada CNC Frezeleme işleminde GG25 gri dökme demirin karbür uçlarla işlenebilirliği araştırılmıştır. Kesme parametreleri ilerleme hızı, kesme derinliği ve kesme hızı olarak seçilirken, çıkış parametreleri yüzey pürüzlülüğü, kesme kuvveti ve güç tüketimi olarak seçilmiştir. Deneyin tasarımı için Taguchi L27 tam faktöriyel kullanılmıştır. Toplam 27 deney yapılmış ve sonuçları analiz etmek için yanıt yüzey metodolojisi (RSM) ve varyans analizi (ANOVA) kullanılmıştır. Ayrıca araştırma çıktılarının daha verimli hale getirilmesi için CNC freze makinesinde talaşları çıkarmadan optimum koşullarda çalışabilmek için bilyalı çubuk testleri yapılmıştır. Bu çalışmanın sonuçları, ilerleme hızının ardından kesme derinliğinin çıktı parametreleri üzerinde en önemli etkiye sahip olduğunu göstermiştir. Deney verilerine göre, ilerleme hızı, kesme derinliği ve kesme hızı arttıkça, güç ve kuvvet de artmaktadır. Yüzey pürüzlülüğü belirleme katsayısı %96,58'dir. Kesme kuvveti ve güç

tüketimi sırasıyla %97,65 ve %91,78 doğrulukla modellenmiştir. Besleme oranı %82,37 ile yüzey pürüzlülüğünde en etkili faktördür. Kesme derinliği sırasıyla %68,82 ve %49,34 ile hem kesme kuvveti hem de güç tüketimi için en önemli faktördür. Yüzey pürüzlülüğü, kesme kuvveti ve güç tüketimi sonuçları için hata yüzdesi sırasıyla %3.42, %2.35 ve %8.22 olarak hesaplanmıştır.

Deney sonunda çıktılar MiniTAB ile formüle edilmiş, deneysel ve teorik sonuçlar karşılaştırılmıştır. Sonuç olarak, tüm tepkiler GG25 gri dökme demir için geliştirilen model kullanılarak tahmin edilebilir. Benzer şekilde, deneysel sonuçlara yaklaşmak için ANSYS dinamik analizi kullanılmıştır. Çalışmanın GG25 gri dökme demirin işlenebilirliği ve işleme yöntemleri ile ilgili literatüre katkı sağlayacağı düşünülmektedir.

Anahtar Kelimeler: GG25 Gri Döküm Demiri, Karbür Kesici Uç, Yüzey Pürüzlülüğü, Kesme Kuvveti, Güç Tüketimi, Tepki Yüzeyi Metodolojisi, ANOVA.

With all my love, I dedicate my efforts to my mother,

my family and all people who prayed for me and supported me

ACKNOWLEDGMENTS

Before anything else, I would like to express my gratitude to everyone who supported me through this academic research. My family, friends, colleagues, and academic mentors have been my source of inspiration, providing me with the determination and support to complete my research project successfully. I sincerely thank the University of Turkish Aeronautical Association for their invaluable aid and guidance.

During the this research, as the author, I would like to express my gratitude to my supervisor, Assoc. Prof. Dr. Suat DENGİZ, and co-supervisor, Assoc. Prof. Dr. Muhammed ARAS, for providing valuable advice, constructive criticism, encouragement, and insightful perspectives. Additionally, I would like to extend my appreciation to all those who provided technical assistance, offering helpful suggestions and remarks. Also, I would like to express my deep gratitude to my brother: whose advice, support, encouragement, sacrifice, and inspiration were instrumental throughout this research.

I am incredibly grateful for my dear mother, who has always been there for me with her prayers, patience, advice, and unwavering support since childhood. Her love, loyalty, and genuine dedication have played a significant role in helping me get to where I am today.

Additionally, I would like to express my gratitude towards my beloved sister for her unwavering encouragement and support throughout my journey.

I wish to express my gratitude for the support and assistance provided by the company of my previous employment during the process of experimental tests and data analysis for the present investigation. The contributions made by my past colleagues are highly valued.

I am incredibly grateful to Assoc. Prof. Dr. Emine Deniz TEKİN from UTAA and Assoc. Prof. Dr. Erdem ÇİFTÇİ from Gazi University for their advice and support and for their assistance in eliminating all the difficulties.

Despite my efforts to compile a comprehensive acknowledgment list, I am aware that I may have unintentionally left out some who may feel left out. I am deeply appreciative, grateful, and humbled by everyone who contributed in any way possible.

TABLE OF CONTENTS

LIST OF TABLES

LIST OF FIGURES

LIST OF ABBREVIATIONS

ANN: Artificial Neural Network

ANOVA: Analysis of Variance

BUL: Built-up Layer

CAD/CAM: Computer-Aided Design/Computer-Aided Manufacturing

CBN: Cubic Boron Nitride

CNC: Computerized Numerical Control

DIN : Deutsches Institut für Normung

DOE: Design of Experiment

FCC: Face-Centered Cubic

GG25: Gray cast iron

HPC: High-Speed Cutting Process

HRC: Hardness Rockwell C

HSM: High-Speed Machining

IMSR: Institute of Management Studies and Research

ISO: International Organization for Standardization

KNN: K-Nearest Neighbor

MRR: Material Removal Rate

OM: Optical Microscopy

RPM: Revolution per Minute

RSM: Response Surface Methodology

SEM: Scanning electron microscope

LIST OF SYMBOLS

a_p: Depth of Cut

f: Feed Rate

N: Newton

R: Cutting tool radius

R_a: Arithmetic Average Roughness

R_i: Ideal average surface roughness

R_q: Root of arithmetic mean deviations

R_t: Sum of maximum height and maximum depth

R_z: Average of the highest five and the lowest five points

V_c: Cutting speed

W: Watt

CHAPTER 1

1. INTRODUCTION

1.1. Motivation and Problem Definition

There has been considerable growth in research and development studies on the quality of the machining process globally during the last several years. There are now some new standards in place for identifying the characteristics that influence metal cutting performance. Cutting inputs such as cutting speed, depth of cut, and feed rate are the fundamental factors for machining. However, two other essential aspects influence the quality of metallic parts. These two factors are the type of raw material and the hardness of the materials.

In recent years, the quality of products in the developing industry has been increasing. It is necessary to consider many factors to improve the components' quality. Cutting speed, depth of cut, feed rate, and cutting tools are primary factors that affect the quality of components. However, if it is desired to increase the quality of the part entirely, attention should be paid to the type and hardness of the material.

The quality of the process, ease of machining, and precision of the final product are all influenced by the structure of the base material. The material's hardness may not be sufficient or even appropriate for metal machining applications. It is necessary to use the heat treatment technique in these situations to obtain the desired hardness. In specific cases, these enhancements are commonly employed. For example, heat treatment is crucial in manufacturing bearing steel. Following the final hardness of the material, appropriate cutting tools should be chosen. In the manufacturing industry, selecting suitable cutting tools depending on the hardness of a material is critical for reliable machining.

Gray cast iron's exceptional wear resistance and thermal conductivity properties make it an important material in many fields. The machinability of GG25 gray cast iron

significantly influences the determination of the efficiency and cost-effectiveness of machining processes.

Various factors, including the morphology of graphite, the structure of the matrix, and mechanical properties, impact the machinability of gray cast iron. To improve the understanding of the machinability of GG25 gray cast iron, a series of empirical tests were carried out, utilizing various cutting parameters and tool geometries. The present study comprehensively examines the experimental results and introduces innovative perspectives on the machinability characteristics of GG25 gray cast iron.

1.2. Background, Workbench Proposed Methods, and Models

In today's world, machining is essential in producing various products. The parts coming from the casting are presented to the user by removing the chips by different methods, such as turning and milling, in order to make them suitable for the customer. These methods used in chip removal must be kept within the required tolerance range. It can be both geometric tolerances and surface response.

Before machining, the ballbar test was performed to observe the current state of the CNC Milling and to determine the geometric tolerance ranges for machining. The ballbar test provides information on whether the machine needs maintenance. First, the engine block was prepared and poured into a sand mold. Then the block removed from the mold was prepared for processing. Afterward, the ballbar test was performed to observe the current state of the workbench.

The cutting tool was chosen as tangential indexable coated carbide inserts, and in-micron size measurements were performed on mounting the cutting tips on the tool holder. The cutting parameters were determined according to the previous studies and based on the machined material. The design of the experiment (DOE) was created with the Taguchi Method, and machining combinations were determined. Then cutting operations were performed, and the output parameters such as surface roughness, cutting force, and power consumption were obtained. These results were analyzed with

input parameters feed rate, depth of cut, and cutting speed using RSM and ANOVA. The link between numerous machining factors and one or more response variables is investigated using the Response Surface Methodology (RSM). According to the results, the data were formulated by approaching the experimental outputs via MiniTAB.

1.3. Contributions and Novelties

Many parameters affect the CNC milling process, and previous studies have investigated the behavior of stock removal for different materials. However, the number of studies that examined the machinability of GG25 gray cast iron is limited.

This thesis will contribute to the literature on the machinability of GG25 gray cast iron material with the formula obtained by the author from the experimental test results.

The followings are the novelties and contributions:

- A minimal number of works can be implemented in a beneficial way in line with GG25 gray cast iron.
- No study has performed a Ballbar test on the condition of the bench, considering that it may vary from CNC Milling operation to machine.
- There is no study in the literature with micron size measurements on mounting the cutting tips on the tool holder.
- Optimum cutting parameters are obtained for machining of GG25 gray cast iron using carbide inserts, which contributes to the future works for this material.

The primary objective of this study is to make novel contributions to the field of machining through a comprehensive investigation of the machinability of GG25 gray cast iron. The research presented in this study possesses novelty and significance as it contributes new insights and knowledge to the field of machining.

This research provides a comprehensive analysis of the machinability characteristics of GG25 gray cast iron. It presents novel findings that contribute to the existing knowledge base in this particular field of investigation. The study highlights the significance of both technological advancements and practical implications, emphasizing their contributions. The following statements clarify the distinctive components and the importance of the study.

Further investigation should be conducted to enhance the understanding of the machinability characteristics of GG25 gray cast iron. The study's notable contribution lies in its emphasis on GG25 gray cast iron, a material that has yet to receive much attention in previous investigations regarding machinability. Despite the widespread utilization of gray cast iron in industrial settings, there exists a need for more empirical data specifically related to GG25. The study activities aim to fulfill a crucial requirement for conducting comprehensive research on the machinability of GG25 gray cast iron, thereby bridging this existing gap in knowledge.

The study sets itself apart from prior theoretical or simulation-based investigations by employing an empirical methodology. The researchers conducted a sequence of machining experiments encompassing turning, milling, and drilling operations, intending to replicate real-world machining scenarios. The investigation yields reliable and practical insights into the machinability of GG25 gray cast iron by means of direct measurement and analysis of cutting forces, surface roughness, and power consumption.

The investigation comprehensively analyzes machining performance, considering various aspects such as cutting forces, surface roughness, and power consumption, among others. This comprehensive examination clarifies how the material reacts to different machining procedures and variables. The investigation has yielded empirical

data that offers a thorough understanding of the distinctive machinability characteristics associated with GG25 gray cast iron.

The comprehensive analysis conducted in this study on the machinability of GG25 gray cast iron yields novel insights in the field, as demonstrated by the findings presented. In conclusion, this study contributes to the scholarly dialogue surrounding the subject matter. Applying the empirical methodology, in conjunction with a thorough analysis of machining efficiency, cutting instruments, and the enhancement of machining variables, addresses a gap in understanding and provides practical viewpoints. Research plays a crucial role in enhancing industrial efficiency, reducing costs, and enhancing the competitiveness of applications that involve GG25 gray cast iron.

1.4. The Objective of the Study

The machining process has a necessary high impact on every part of the industry. In fact, cast and machined parts are used in many aspects of daily life. For example, the differences in the problems experienced in the engine block of the vehicles used by many people to get from one place to another daily are based on the processing and casting method. This study it is aimed to reach the optimum levels of the cutting parameters in the machining of GG25 gray cast iron.

1.5. The Outline of the Thesis

Chapter 1

In this chapter, as an introduction, motivation, and problem definition, proposed methods and models, contributions, and novelties aim of this study of the machining process are presented with a clarification of the thesis outline and work structure.

Chapter 2

A review of all studies related to the subject is discussed by dividing the research according to the work of the respective researchers in these studies.

Chapter 3

The experimental work, insert type, methodology, CNC milling, ballbar test, cutting force, power consumption measurement, and surface roughness measuring are explained in this chapter. Several tests are being made to ensure the results.

Chapter 4

This chapter presents the results with figures of the simulation analysis and experimental work with a discussion of the results and analysis.

Chapter 5

Finally, the study's conclusion and work are revealed, followed by possible future academic works and recommendations.

1.6. Thesis Structure

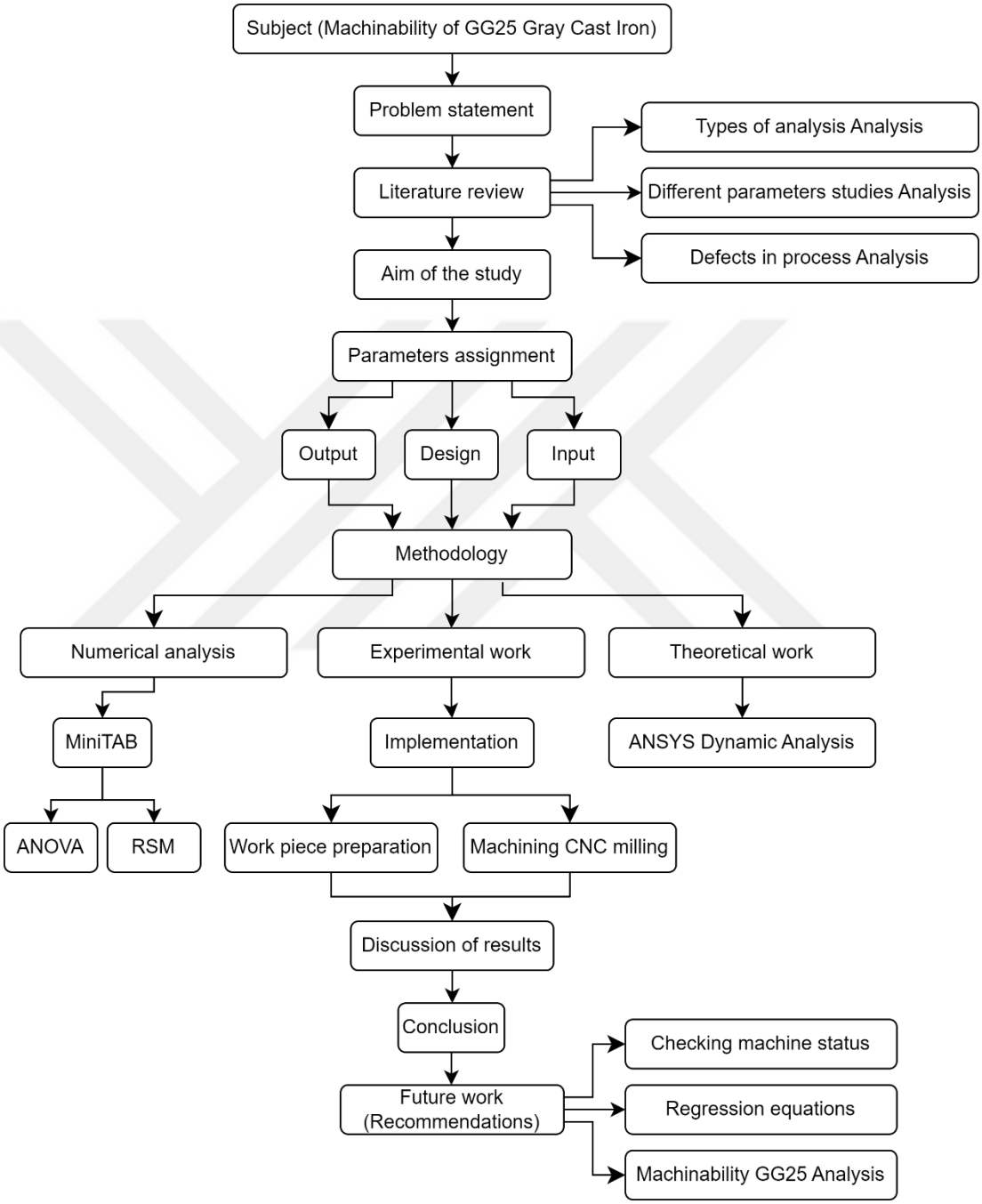

CHAPTER 2

2. LITERATURE REVIEW

Researchers are currently addressing the challenges associated with manufacturing and industry, such as the need to produce high-strength components, resistance to fatigue and corrosion, improved surface polish, and reduced processing time and cost. GG25 gray cast iron is a material frequently used in all areas of industries. It is currently the preferred material, especially in the engine block. In this section, studies on the processing of GG25 material are examined, and literature reviews are compiled.

GG25 gray cast iron is one of the most preferred materials in the industry. It is composed of 3.00 to 3.25% carbon, 1.85 to 2.10% silicon, 0.4 to 0.7% manganese, a maximum of 0.12% sulfur, a maximum of 0.25% phosphorus, and iron balance compounds. It has 123 MPa tensile strength, 159 HV hardness, and 7.2 J/mm^2 impact toughness. Due to its castability, resistance to corrosion, machinability, low melting point, cost-efficiency, and superior damping capability, gray cast iron is a common industrial material. It is frequently used to manufacture machine parts such as hydraulic valves, engine blocks, and disc brake rotors [1]. The graphite flakes that form during solidification and give gray cast iron its low strength and toughness are primarily responsible for controlling its mechanical properties. The microstructure of gray cast iron is characterized by the distribution of graphite lamellas in the ferrous matrix [2]. The processing of this material is essential as it is the optimum material to be processed in terms of machinability-customer balance and desired material properties. The following studies have already been carried out on this material.

Taşliçukur et al. investigated structural and conductive analysis of GG20 and GG25 materials. Accordingly, in the research, first of all, the structure of graphite was examined through microscopes, and matrix phases were obtained with the help of light and electron microscopy. In the second stage, tests were carried out at room temperature to determine the durability of the obtained matrix phases, and the Charpy

impact test was performed. As a final step, fractographic analysis was performed. The reason for this is to examine the fracture behavior of the matrix excess obtained in the previous tests and the materials subject to the research against temperature. The findings show that layer gap and carbon content directly affect the materials. Although GG20 material has a higher hardness and strength than GG25 material, the impact toughness of GG25 material is higher than GG20. The reason for this is the higher amount of graphite in the matrices. In addition, GG25 and GG20 materials also have very high graphite values and pearlitic matrices. When viewed as a ratio, it was determined by the authors that GG20 material had higher graphite values with the applied image analysis [1].

Martinho et al. investigated the effect of cutting speed and feed rate on the cutting force and wear analysis in high-speed machining of gray cast iron using ceramic tools with and without diamond coating. In this study depth of cut is kept constant (1 mm) while cutting speeds are selected as 500, 700, and 900 m/min, and feed rates are chosen as 0.1, 0.25, and 0.4 mm/rev. The results were collected with homemade software and correlated with rational decisions. It was found that an increase in the main cutting force was associated with an increase in the feed rate. High temperatures often occur in the cutting zone while high-speed machining (HSM). Therefore, chemical and diffusion reactions, such as the adhesion of iron and manganese between tool and workpiece material, have been observed [3].

Yuhai analyzed the production methodology about the condition of diamond tools, cubic boron nitride cutting tools, and coated tools during high-speed machining. The utilized material is GG25, while the cutting tools employed are CBN 30 and CC650 ceramic. The cutting parameters used in this study include a depth of cut of 2.5 mm, a feed rate of 0.3 mm/rev, a cutting speed of 400 m/min, and a tool life of 550 pieces. This study examines the factors affecting the wear life of high-speed cutting tools utilized in various applications. The findings provide valuable guidance and reference for the rational selection of high-speed cutting tools and their wear during actual machining. The study aims to provide a comprehensive analysis of the advancements

in high-speed machining technology and the enhanced performance of PCBN diamond tools [4].

The machinability of EN-GJL-250 gray cast iron was investigated by Vopát et al., focusing on the tool life of coated carbide cemented drills. The cutting parameters utilized in this study were a cutting speed of 100 m/min, a feed rate of 0.4 mm/min, and a depth of cut of 5.75 mm. This study primarily focuses on the categorization of advanced microgeometry within the field and evaluating its significance. The present investigation involved acquiring and comparing life data about the edge materials of cemented drills and the machining outcomes observed prior to and after the alteration of the cutting-edge radius. The carbide materials underwent a cement coating process followed by a subsequent coating with TiAIN. The findings indicate that there is a positive correlation between the cutting radius size of cement-coated tools [5].

Martinho et al. obtained a theoretical study using diamond-coated and uncoated tools in machining gray cast iron called DIN GG25. The cutting depth was kept constant (1 mm) during this process. Afterward, nine-speed combinations with 500, 600, and 900 m/min and feed with 0.1, 0.25, and 0.4 mm/rev were used. According to the results, it was observed that the wear phenomenon on the ceramic tips is both chemical and mechanical. Abrasion, adhesion, and diffusion were observed in ceramic tools without any coating and coated with 15 μm thick diamond film tools. SEM and optical microscopy were used to measure worn and chipped surfaces. According to optical microscopy data, it has been observed that the tool life of diamond-coated inserts is longer than the tool life without coating [6].

Fiorini et al. investigated the mechanical effects of a high-speed cutting process (HPC) on gray cast iron. The high-performance cutting process maximizes product performance while it is minimizing production time. It provides optimization of product quality. According to the research results, When the HPC process was examined in terms of gray cast iron processing, they observed a serious reduction in the processing time by preserving the product quality in terms of surface quality. For this reason, the necessity of using HPC as a cutting force for energy efficiency and shortening the energy production process has been emphasized as a solution [7].

Saligeh et al. reported the effects of surface wear and shear forces on bimetallic composites. Bimetallic parts made of aluminum and cast iron are machined in face milling. Bimetallic parts are used in many industries to reduce costs and workload. The automotive industry is the largest sector where these materials' effects are seen. Different machining conditions such as depth of cut 1.5 and 2 (mm); feed rate 100 and 125 (mm/min); cutting speed 500, 800, and 1250 (RPM) used to calculate tool wear area using K-Nearest Neighbor (KNN) image processing method. Tool wear area resulted as 0.103, 0.23, and 0.26 (mm^2) for bimetallic parts; 0.09, 0.098, and 0.108 for cast iron. Cutting speeds 250, 800, and 1250 (RPM); feed rates 100, 125, and 80 (mm/min) are machining parameters for cutting force measurement experiments, respectively. Average resultant force for cast iron 115.28, 59.28, and 30.28 N; aluminum 153.37, 72.23, and 44.74 N; and bimetallic parts 145.01, 90.24, and 68.78 N for specific machining conditions. In the tests performed, the machining length of 3.6 m was used, and wear was observed on the side surfaces of the alloys. According to the test results, it has been observed that the parts on the side surface are not significantly worn compared to the cast iron and bimetallic surface wear, and the wear and tear rate of the bimetallic parts is much higher than the cast iron [8].

Padmakumar et al. compared the wear of cryogenically treated and untreated tungsten carbide inserts during face milling of gray cast iron, which is a popular material for machine tool beds and automotive components due to its low cost, high vibration damping capability, and ease of manufacture. The study used commercially available uncoated tungsten carbide implants with a Co concentration of approximately 6%. The performance evaluation criteria were flank wear and nose wear. The results reveal that cryogenically treated and tempered inserts have a longer tool life than untreated inserts, which may be attributed to Co's martensitic phase shift from -Co (FCC) to -Co (HCP) and the creation of compressive residual stress in the treated insert samples. The magnetic saturation and coercivity of the untreated and treated samples were studied using metallographic techniques for validation. Consequently, the authors found an average of 20% less flank wear than the untreated inserts and 12% less nose wear than the untreated inserts [9].

According to this experimental study by Fiorini et al., the effectiveness of high-speed machining of gray cast iron is linked to the protective built-up layer (BUL) that forms on the tool. Besides, BUL formation on PcBN tools for dry, high-speed machining of GG25 gray cast iron (up to V_c = 750 m/min) is investigated. This research reveals that at high cutting speeds (V_c = 750 m/min), the BUL distribution on the tool is critical for tool safety. At low cutting speeds (V_c = 250 m/min), protection in the area of maximal cutting temperature is crucial in minimizing thermally induced wear types like crater wear [10].

Gray cast irons are often used in machine tools due to their low cost, good vibration-dampening capability, and ease of manufacture. The range of tensile strength and form of graphite establish the classes of these alloys, which are determined by the guiding requirements for their manufacturing. This investigation aims to conduct a comparative analysis of the machinability of two gray cast irons from the same class within the same standard tolerance but with varying pearlitic/ferritic concentrations. Using carbide and ceramic tools and two distinct cutting speeds, machinability was assessed regarding tool life and cutting pressures in milling operations. Two different materials were used as samples: one with 100% pearlite and the other with 50% pearlite and 50% ferrite. The findings revealed that milling the 100% pearlitic alloy resulted in quicker tool wear and greater cutting pressures than milling the 50% ferritic alloy. The life of ceramic tools was significantly longer than that of carbide tools. Diffusion, attrition, and thermal fractures were reported as wear processes. On the other hand, the material microstructure was shown to be considerably more critical than the other input factors, such as cutting speed and tool material for tool life and cutting force [11].

In this paper presented by Lacalle et al., optimum conditions of high-speed machining are aimed at industrial application techniques. The material was chosen as GG25 gray cast iron and GGG70L ductile cast iron. Tools made of polycrystalline cubic boron nitride (PCBN) and coated carbide were used in the test. For tools made of coated carbide, the cutting speed may reach 140 m/min, while PCBN can reach over 300 m/min. Coated carbide tools exhibit greater hardness but have relatively low wear

resistance. The paper concludes by stating that HSM may reduce manufacturing timelines in the stamping die by 7% to 10% while improving machined products' quality. As a result, delivery times may increase, and the business's competitiveness can be raised [12].

Malakizadi et al. used SEM to examine the CBN inserts' wear mechanism during the face milling of an aluminum-gray cast iron engine block. They mimicked face milling in real-world settings using the Finite Element Method (FEM). The inverse approach was used to estimate the yield stress characteristics of gray cast iron and aluminum-silicon alloy, and the milling process was independently modeled for each material to get thermally and mechanically generated stresses at the tool edge. Thermal cracking has been demonstrated to be the primary wear mechanism for CBN inserts used in the face milling of bimetallic engine blocks. Under identical cutting conditions, it was found that gray cast iron's temperature during machining was about twice as high as aluminums'. This study's technique may be used to identify the ideal tool microgeometry, cutting circumstances, or both for long tool life and little wear development [13].

In Özbeyaz's study, the impacts of the key factors on the surface roughness values are examined. The artificial neural network (ANN) based prediction model is created using the MATLAB toolbox. Aluminum 1050 blocks are employed as a workpiece material, and the impact of the three milling parameters on the surface roughness is investigated. In this study, 1000, 2000, and 3000 RPM are used as cutting speeds, 420, 840, and 1260 mm/min are chosen for feed rates, and 0.3, 0.6, and 0.9 mm are selected for depths of cut. For a 2000 rpm cutting speed, a 420 mm/min feed rate, and a 0.3 mm depth of cut, the minimum Ra is measured as 0.2910 µm. With a cutting speed of 1000 rpm, a feed rate of 1260 mm/min, and a depth of cut of 0.9 mm, the maximum Ra is calculated to be 1.4943 µm. The main element influencing surface roughness is the feed rate. The surface roughness will often rise if the feed rate is routinely increased. On the other side, a higher feed rate and lower cutting speed would result in more excellent surface quality. Finally, the coefficient of determination is calculated as

98.7%, and the mean square error from all 18 experiments is -0.0015, which is small enough for predictions [14].

Thamizhmanii and Hasan studied the effect of input parameters on the surface roughness, cutting tool forces, and tool wear in the turning of gray cast iron. In this study, a constant depth of cut was used with 0.5 mm, various cutting speeds of 23, 45, 100, and 135 m/min, and different feed rates of 0.08, 0.1, 0.125, and 0.16 mm/rev. At feed rates of 0.08 and 0.10 mm/rev, the cutting force exhibited a low magnitude. In contrast, the cutting force displayed an initial low value, which subsequently escalated with an increase in the cutting speed. However, the magnitude of the radial force observed in each experiment was relatively low. The magnitude of vibration is expected to be higher along the cutting force direction as compared to the radial force direction. They stated that the surface roughness is dropped at a higher cutting speed and feed rate. Also, flank and crater wear occurred on the cutting tool during turning [15].

Souza et al. examined the surface roughness, tool wear, temperature, and cutting forces during turning gray cast iron with a silicon nitride-based ceramic insert. Increasing the feed rate raises both cutting force and surface roughness. The study involved conducting experiments at various cutting velocities ranging from 180 to 420 m/min while maintaining a constant depth of cut of 1 mm. The feed rates used in the experiments were 0.12, 0.23, 0.33, 0.40, and 0.50 mm/rev. The cutting procedure was executed on two occasions for each given condition. The original construction material was cylindrical, featuring a diameter measuring 105 mm and a length of 300 mm. Following every pass on the cylindrical workpiece and until the tool's end-of-life, three surface roughness measurements were acquired at 120-mm intervals. The statistical measures of mean and standard deviation were computed for the surface roughness variable at every cutting speed. However, as the cutting speed rises, the surface roughness drops while the cutting forces and the temperature lead. Finally, the tool wears sharply as the cutting length increases [16].

Bağcı's study proposes a novel and exact method for estimating cutting parameters and optimizing feed rate to maximize productivity during freeform milling surfaces.

The cutting edge is B-spline curves, while the workpiece and material removed are both represented using solid models. Second, in the virtual manufacturing environment, the feed rate that significantly affects the precision machining of freeform surfaces is optimized and improved. This technique for accurate calculation of instantaneous and average material removal rate (MRR) values, effective cutter diameter values, chip thickness, chip volume, surface form errors, and cutter-workpiece contact area. In the creation of freeform surfaces, the suggested feed rate optimization approach dramatically decreased cutter deflection, cutting forces, and surface form defects [17].

Karakus used a four-axis horizontal machining facility to examine the milling behavior of exhaust manifolds and the effects of various factors, including surface roughness and noise level. Using constant cutting speeds of 120, 240, and 360 m/min, various feed rates of 0.20, 0.40, and 0.60 mm/rev, and various depths of cut of 0.5, 0.75, and 1.5 mm, empirical investigations were conducted in a real machining environment. The effect of the milling parameters on surface roughness and noise level was investigated using the statistical data analysis application MINITAB. In conclusion, increasing the feed rate and depth of cut notably affected surface roughness [18].

In this field, it can be observed that a few studies discussed the different parameters that affect the machinability of GG25 gray cast iron, and the number of studies that address numerical analysis with this process is limited. This study presents some new aspects, such as: (1) This is the first study to demonstrate the ballbar test process. (2) The mathematical models were developed to predict the responses. (3) No research has discussed the machine's condition before and after the experiment. (4) This study is the first to compare the theoretical and experimental results of the processing of the engine block in a complex structure. (5) Multiple measurement processes have been completed in order to obtain good results in each region. (6) ANSYS metal removal analysis, ballbar tests, measuring machine for tool optimization with insert, and mathematical analysis with MiniTAB all in one have never been used in any study before.

CHAPTER 3

3. MATERIAL AND METHOD

This study examines the machinability of GG25 gray cast iron with carbide inserts on a CNC Milling Machine. The effect of various cutting parameters such as feed rate, depth of cut, and cutting speed is investigated on the surface roughness, cutting forces, and power consumption using Response Surface Methodology (RSM). In addition, ballbar tests are carried out to work in optimum conditions without removing chips in the CNC Milling machine to make the research outputs more efficient. Analysis of variance (ANOVA) is used to determine the most influential parameter on the responses. Besides, regression equations are developed to predict the outputs considering the different combinations of cutting parameters for the machining of GG25 gray cast iron. The study will contribute to the literature regarding the machinability and processing methods of GG25 gray cast iron.

3.1. Material

Gray cast iron is a popular industrial material because of its castability, corrosion resistance, machinability, low melting point, low cost, and excellent damping capacity. It's commonly used in the production of machine parts, including engine blocks, disc brake rotors, and hydraulic valves [19,20].

The mechanical qualities of gray cast iron are controlled mainly by graphite flakes, which develop during the solidification process and give low strength and toughness. Graphite lamellas distributed in the ferrous matrix describe the microstructure of gray cast iron. Primarily related to the basic material structure, the quantity of graphite present and the size, shape, and distribution of graphite lamellas are essential factors in influencing mechanical behavior [21,22]. This material structure provides the

extraordinary damping ability of gray cast iron, which is much higher than steel or other types of cast iron, which may be due to the flake graphite structure [23].

Most of the carbon in gray cast iron, also known as flake graphite cast iron, is flake graphite. The distribution, size, and number of graphite flakes and the matrix structure influence the qualities of gray cast iron [24]. The chemical composition and mechanical properties of GG25 gray cast iron are given in Tables 1 and 2, respectively.

The selection of GG25 gray cast iron as the test material was determined by its widespread use and significance in various industrial situations. An analysis was conducted on the chemical composition and microstructural characteristics of GG25 to ensure accurate representation.

Table 1: Chemical composition of GG25 gray cast iron [25]

Materials	C %	Si %	Mn %	S %	P %	Fe %
GG25	3.00-3.25	1.85-2.10	0.40-0.70	max. 0.12	max. 0.25	balance

Table 2: Mechanical properties of GG25 cast iron [26]

Materials	Tensile Strength, MPa	Hardness, HV10	Impact Toughness, J/mm^2
GG25	123	159	7.20

3.2. Cutting Parameters

In order to process the material, cutting speed (V_c), feed rate (f), and depth of cut (ap) must be determined. Table 3 shows the cutting parameters which are selected based on the previous studies and the recommendation of the cutting tools manufacturer. In the experiment, carbide-cutting tools were used. The Taguchi method aims to see the different factors and their relationships with the least experiments and interpret them statistically. In the MiniTAB program, minimum cutting speed, feed rate, and depth of cut values were reached using the Taguchi Method. Then the data was analyzed with the help of ANOVA.

The study carried out an empirical test to evaluate the machining performance of GG25 gray cast iron. The test measured cutting forces, surface roughness, and power consumption. The study performed comparative analyses to evaluate the effect of different cutting parameters on machinability.

Table 3: Cutting parameters

Cutting Parameter	Unit	Level		
		1	2	3
Depth of cut, a_p	mm	0.1	0.3	0.5
Cutting speed, V_c	m/min	300	500	700
Feed rate, f	mm/min	2000	3000	4000

3.3. Cutting Tools

Tooling manufacturers are under constant pressure to provide innovative products that can resist the heat produced during the cutting process while extending tool life due to the growing usage of difficult-to-cut materials. The tool's cutting edge may be affected by the high temperatures in the cutting zone, which can cause plastic deformation and shorten tool life. A coating on the carbide inserts increases wear resistance and the amount of material a single insert may remove. Higher machining speeds may often be attained as well. Coatings create a barrier to chemical interaction between the substrate and the substance of the workpiece. Coatings are tough, improving wear resistance. By assisting in preventing wear modes, coatings increase tool life.

The thermal barrier that coatings produce prevents heat from entering the substrate. Compared to conventional cutting tools, indexable inserts have a substantial benefit in that a worn cutting edge is transformed into an unused cutting edge, eliminating the requirement for regrinding. This guarantees that production is only momentarily stopped and eliminates the need for a time-consuming tool setup. The production type, the machining material, and its hardness level will all affect the cutting insert to choose.

Numerous company owners, construction workers, and many others worldwide find carbide inserts to be of great use. Comparable tools are less expensive and less effective than carbide inserts. Because of its exceptional durability, carbide material has a substantially longer functional life. There are more than a dozen grades of tungsten carbide, all of which have diverse uses. Tungsten carbide materials yield a substantially superior surface finish quality when used as cutting tools. Additionally, tungsten carbide inserts and other carbide recycling materials have a wide range of applications, making them crucial components for several industries.

A heat barrier is crucial in high-speed procedures where plastic deformation is the main issue. Today's inserts typically come in coated carbide grades, around 80%. They enable machinists to boost metal removal rates and cutting speeds while significantly extending tool life compared to uncoated inserts. Indexable inserts are standardized worldwide to avoid making the wrong choices. The size, form, mounting, material qualities, and coating are all specified by this ISO standardization. Using the ISO indexable insert designation, the cutting machine operator chooses the suitable indexable insert required for the practical application.

The maximum number of characters in an ISO code is twelve. The required information is shown by the first to seventh characters seen in Figure 1. The optional information on the eighth and ninth is utilized as necessary seen in Figure 2. The tenth supplements the ISO code through the twelfth manufacturer information, which is optional and provided independently. The seven required fields list the cutting insert's essential characteristics, such as the clearance angle and insert form. The characters readily distinguish an indexable insert thanks to their unique identifying letters and numbers [27].

An example is given below;

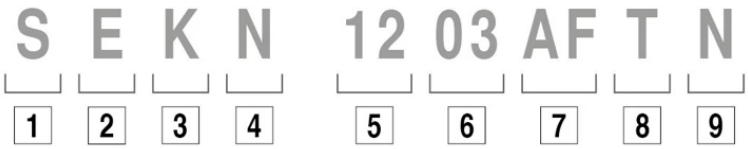

Figure 1: Explanation of cutting insert characteristics

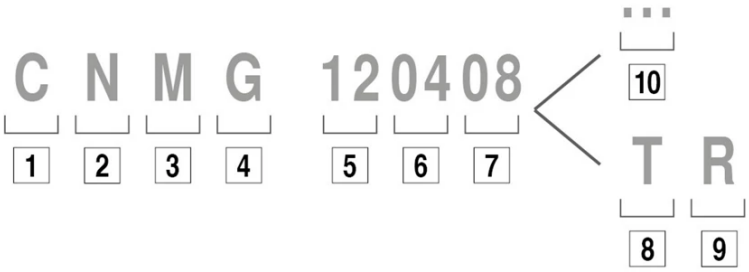

Figure 2: Cutting insert characteristics with manufacturer's information

So that letters and numbers means, 1 = insert shape | 2 = clearance angle | 3 = tolerances | 4 = machining and fixing characteristics | 5 = cutting edge length | 6 = insert thickness | 7 = nose radius | 8 = cut development | 9 = cutting direction | 10 = manufacturer's information. [28]

This study uses Mapal inserts as cutting tools for removing the chips. The technical specifications of inserts are given in Table 4 and from Figures 3 to 5.

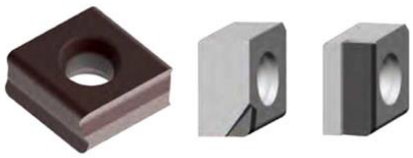

Figure 3: Cutting insert

Table 4: Geometric data of insert

Description	Value
Insert number	CTHQ090504H03R-HP350
Company code	MP - Mapal
Subclass	201-03 - Rhombic insert
Chip breaker face count	0 - Without chip breaker
Chip breaker manufacturers name	H03
Coating	AlTiN
Coolant supply property	0 - Without a coolant supply
Insert included angle	80 Degree
Insert rake angle	10 Degree
Face land angle	8 Degree
Grade manufacturer's designation	HP350
Inscribed circle diameter	9.525 mm
Insert mounting style code	Counter bore for screws with taper angle from 40° to 60°
Insert hand	R - Right
ISO property	0
Corner radius	0.4 mm
Insert thickness	5.56 mm
Insert thickness total	5.56 mm
Standard designation	CTHQ090504R
Tolerance class insert	H

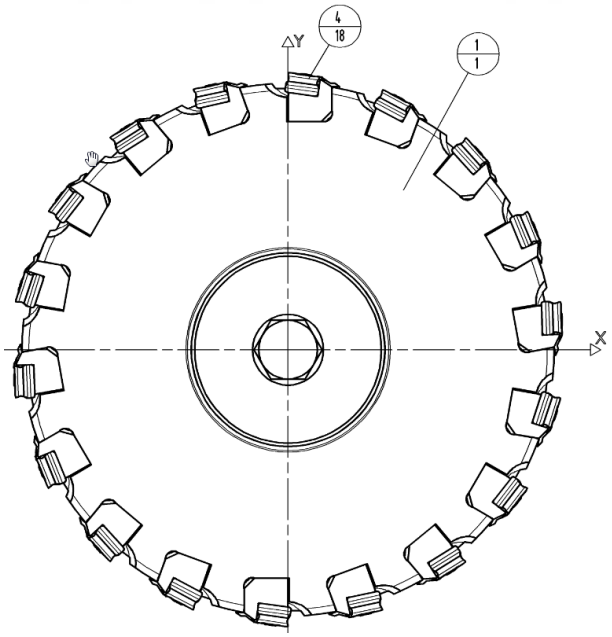

Figure 4: Cutting tool schematic in 2D

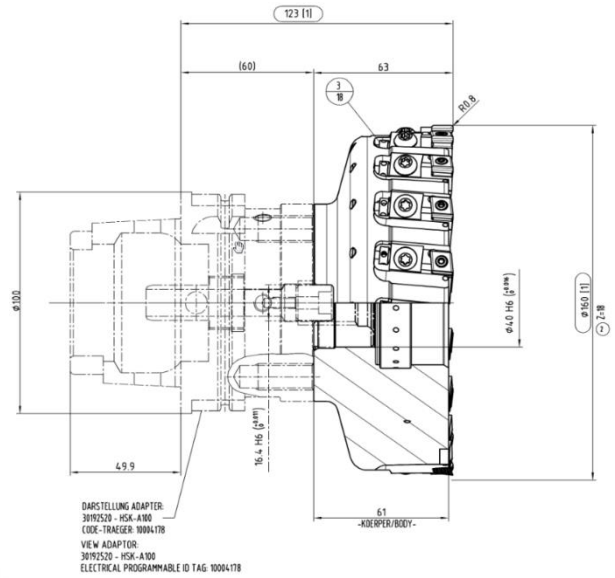

Figure 5: Cutting tool specified specifications with dimensions

The machinability of GG25 gray cast iron is significantly affected by the choice of cutting tools. The work extensively examines different tool materials, geometries, and coatings, highlighting their influence on machining performance.

3.4. CNC Machine

The HELLER MC6000 CNC Milling machine is used in this study for performing the experimental test. The technical properties of this machine are given in Table 5.

Various machining experiments were conducted, employing different cutting tools, machining parameters, and cooling/lubrication methods. The experimental procedures included turning, milling, and drilling operations designed to replicate authentic machining scenarios.

Table 5: Technical specifications of HELLER MC6000 CNC machine [29]

HELLER MILLING CENTER		Unit	MC 6000
Working area	X	(mm)	1000
	Y	(mm)	1000
	Z	(mm)	1000
Progressive Forces	X and Y axis at S3-40% usage time	N	15000
Speeds	Axis dynamics Power Fast feed in X, Y, and Z axis	mm/min	50000
Business Unit Power Cutting	Maximum drive power at S6-40% usage time	kW	43
	Maximum torque at S6-40% usage time	Nm	822
	RPM range	1/min	8000
Team Magazine	Maximum tool size	kg	25
Installation Data	Machine height	mm	4300
	Machine size	kg	13500
	Total working power of the machine	kVA	~40
	temperature range	°C	10_45
Pallet Changing Device	pallet size	mm × mm	630 × 630
Table	pallet height	mm	
ATC	Tool storage volume	set	50/100
	Team size	mm	600
	Tool change time	s	3.6
Performance capacities	Position precision	mm	0.009

3.5. Ballbar Testing Device

This study used Renishaw QC20-W wireless ballbar for CNC milling canter tool performance analysis before and after all tests. Ballbar testing offers a quick and easy way to monitor how well CNC machine tools work regarding positioning by international standards like ISO, ANSI/ASME, etc. Users may also readily detect issues that need maintenance and the sources of mistakes, as well as compare and monitor the performance of the devices.

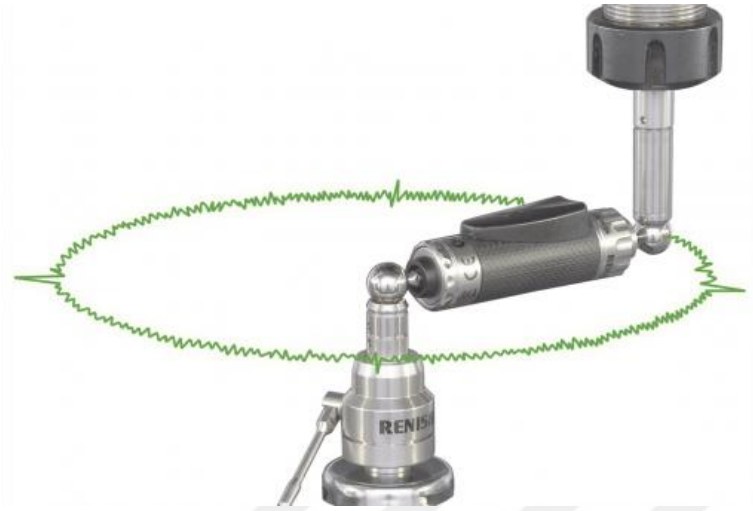

Figure 6: Ballbar test calibration

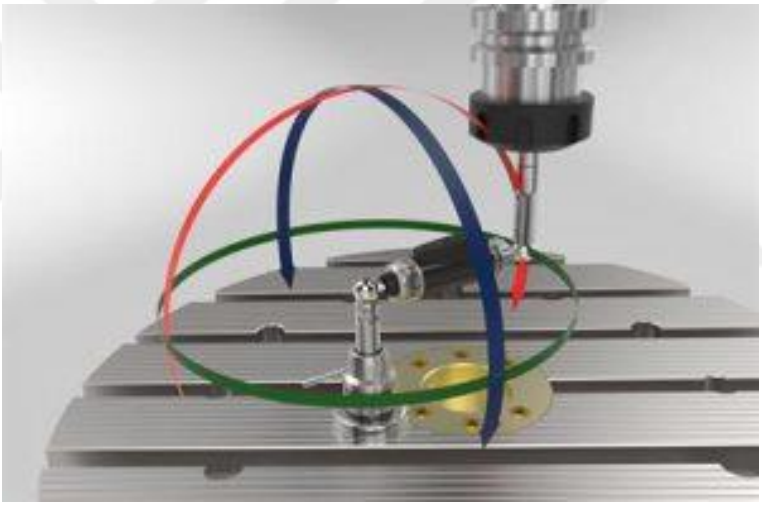

Figure 7: Paths followed during ballbar test measurement

While measuring, the Ballbar test follows the same paths as in Figure 6-7. The working principle compares the data received from the CNC machine with the simultaneous G-code with the distance it travels. So, for instance, when two hundred millimeters of G-code is written in a CNC machine on the x-axis, the probe compares whether it travels 200 millimeters on the x-axis.

The report's findings of outputs Ballbar test include the following elements:

- Ball screw gaps (Backlash)
- Squareness (Scale, perpendicularity, etc.)
- Transverse plays (Wedge, sled, car faults)
- Pitch errors
- Servo mismatches
- Reversal spikes in servo direction changes

3.6. Experimental Method

Recently, optimization has been crucial to the machining sector. The use of progressive optimization techniques, such as response surface methodology (RSM) and Taguchi, can improve the use of machining and assist manufacturers in meeting their intended goals. Previous research has demonstrated that decreasing surface roughness helps minimize workpiece wear, friction, and fatigue [30]. These experiments indicate that the surface roughness value and feed rate reduce. Over the past three decades, research has been done in an effort to create a system that can model surface roughness in accordance with machining parameters. Surface roughness, cutting force, and power consumption in the machining process are influenced by a number of machining factors, including feed rate, depth of cut, cutting speed, workpiece diversity (material and hardness), and tool variety (tool material, cutting edge geometry, chip angle, etc.). Figure 8 shows a 3D sketch of the engine block with the surface to be processed that is used in this study [31].

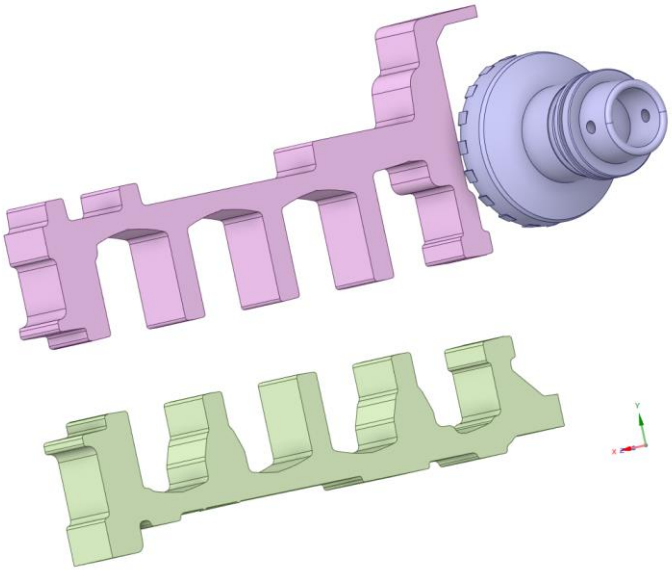

Figure 8: 3D data of engine block and tool

The design of the experiment (DOE) was created using Taguchi L27, and the response surface analysis was performed with MiniTAB analysis, as seen in Figure 9. The model was made, and the input and output parameters were analyzed in response surface design. The L27 Taguchi design was used in the study that was just given to establish a connection between the input and output parameters.

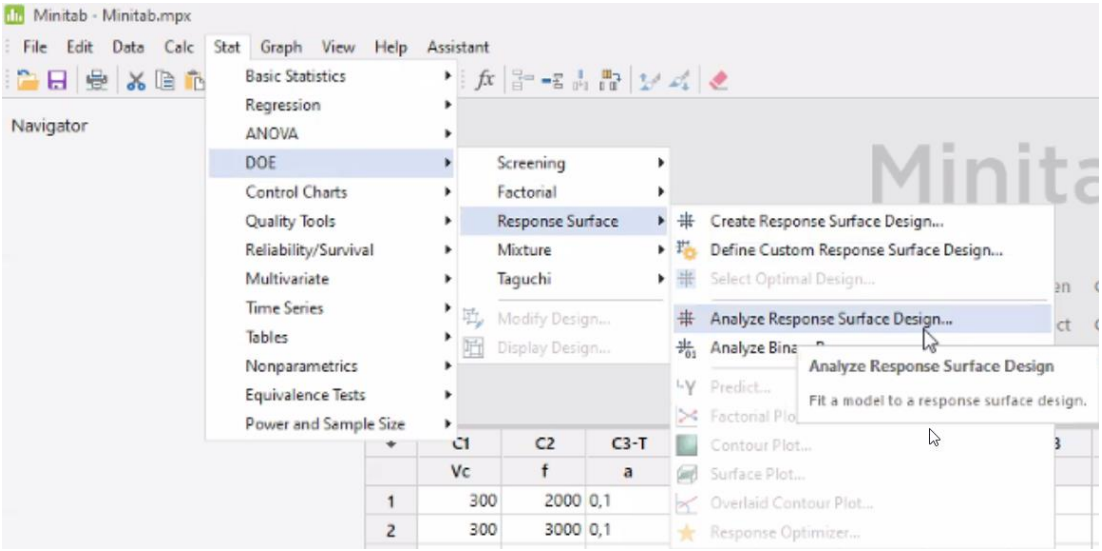

Figure 9: Fitting a model to RSM (DOE)

3.7. Taguchi Method Design of Experiments (DOE)

Dr. Genichi Taguchi is credited with inventing the Taguchi method, also known as the Design of Experiments (DOE). This technique is widespread in the domains of quality engineering and optimization, intending to augment the effectiveness of products or processes while simultaneously reducing variability and susceptibility to uncontrollable factors. The Taguchi methodology is a structured and effective technique that involves three fundamental stages: system design, parameter design, and tolerance design [32].

In the system design phase, the researcher identifies controllable and uncontrollable factors that may impact the performance of the product or process being studied. Design parameters refer to the adjustable factors that the researcher can control while experimenting. Conversely, uncontrollable factors, commonly referred to as noise factors, are independent variables beyond direct control but can impact performance. The parameter design phase aims to identify the most favorable values of design parameters that can achieve the intended performance.

Taguchi method utilizes an orthogonal array, a particular experimental design that effectively assesses the impacts of modifications in design parameters, aiming to achieve the desired outcome. Using orthogonal arrays, researchers can obtain substantial data while minimizing expenses by conducting a restricted number of investigations [33].

The Taguchi methodology incorporates the signal-to-noise (S/N) ratio to assess performance quality. The Signal-to-Noise ratio serves the purpose of measuring the discrepancy between the achieved and intended levels of performance. The approach takes into consideration both the average and the variability of the output. The aim is to optimize the signal-to-noise ratio, which denotes a high degree of performance uniformity and decreased susceptibility to noise [34].

During the tolerance design phase, the researcher establishes the acceptable ranges or tolerances for the design parameters. The previously mentioned stage is of tremendous significance in guaranteeing that the durability and strength of the optimized configuration remain unaltered in the face of fluctuations in manufacturing or operational circumstances. The Taguchi methodology facilitates the attainment of an optimal equilibrium between the intended performance and costs by establishing suitable tolerance levels.

To sum up, the Taguchi method provides a methodical and efficient approach to enhance product or process design. By considering controllable and uncontrollable factors, scholars can ascertain the most advantageous levels of design parameters, augment performance uniformity, and mitigate the influence of extraneous variables. Integrating the Taguchi method into one's thesis can facilitate the enhancement of system or product quality and robustness through the design of experiments and analysis of results.

3.8. Response Surface Methodology (RSM)

The response surface methodology (RSM) is a technique for figuring out how input and output parameters relate to one another. This process has six steps: [35] Surface roughness measuring and desired parameters as R_a result seen in Figure 10.

- Establishing the input and output parameters
- Assuming a design strategy for an experiment
- Regression analysis utilizing the response surface methodology
- Determining the analysis of variance for the input parameters will help you identify the factor that has the highest impact on the output variables.
- Evaluating the RSM findings to determine if the RSM model requires examining variables or not.

In this experimental study, cutting parameters, including feed rate, depth of cut, and cutting speed, were compared with reaction variables like cutting force, power consumption, and surface roughness under dry cutting conditions. A full factorial orthogonal array with three cutting depths, three cutting speeds, and three feed rate values was used for this experimental study. The most effective parameter on surface roughness is the feed rate seen in equations 1-2.

Figure 10: Surface roughness measuring probe

Surface roughness parameters are:

- R_a: Arithmetic mean $R_a = \frac{1}{l}\int_0^l |\, Z(x) \,|\, dx$ (1)
- R_z (JIS): Average of the highest five and the lowest five points
- R_t: Sum of maximum height and maximum depth
- R_q: Root of arithmetic mean deviations

$$R_i = \frac{f^2}{32r} \quad (2)$$

- R_i: Ideal average surface roughness, mm
- f: Feed Rate, mm / rev
- r: Cutting tool radius, mm

3.9. Surface Roughness Measuring

High cutting speed and low feed rates in machining ensure better surface quality. A quality machined surface significantly affects fatigue strength and corrosion resistance. Surface roughness is affected by many factors in machining. Some of these factors can be listed as follows:

- Tool geometry
- Cutting parameters
- Mechanical properties of material and cutting tool
- The status of the machine tool
- Wear the condition of the cutting tool, etc.

Several types of devices can be mentioned to examine the surface roughness. These are electrically operated pointed machines; the touching surface is evaluated, and measuring this situation is with mechanically operated devices, different types of light interference microscopes, and making surface copies.

In this study, a Mitutoyo SJ 210 (178-560-01D) test device was used to measure the surface roughness in Figure 11. Three surface roughness measurement was performed on the machined surface, and the average value is considered the final surface roughness value.

Figure 11: Surface roughness measuring, Mitutoyo SJ 210

3.10. Measuring Cutting Force and Power Consumption

The following information is about the cutting force and power consumption that are automatically calculated during part processing by the CNC horizontal milling machine used in this examination. This information includes the maximum and minimum values. It presents all the data generated during cutting to the user graphically, as shown in Figure 12. By combining these values, our CNC horizontal milling machine, which is used in this study, calculates the data during processing in the form of a block average. This study used the average block value in watts (*kW*) for power consumption. Also, the average block value in newton (*kN*) was sourced for cutting force seen in the figure below radial feed force from the CNC machine. The data received from the CNC machine are in *kN* for cutting force and *kW* for power consumption. In this thesis, Newton (*N*) and Watt (*W*) were used for mathematical calculations.

Figure 12: Cutting force and power consumption graph

CHAPTER 4

4. RESULT AND DISCUSSION

4.1. ANSYS Results

This study analyzed the simplified Beam, Shell, and Solid structures using the Solid 3D structure in Figure 13. The related structure is divided into smaller structures called meshed and discretized with simple elements. Next, the equation describing the relationship between an element and the surrounding node is calculated. Boundary conditions are applied to the model. The element strain and stresses were calculated with the displacements obtained from the solved equations. It is a numerical method that provides solutions by reducing complex engineering problems to simple and small structures. These small and simple structures are called elements. The model consisting of a finite number of elements and nodes is called the finite element model, which is actually an infinite set of points connected to each other through nodes.

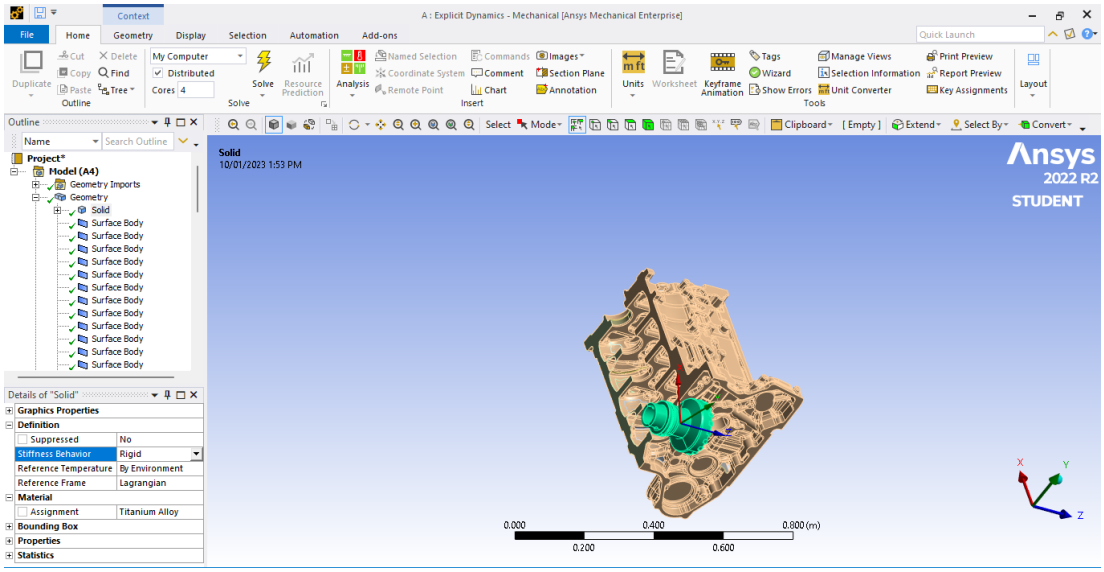

Figure 13: ANSYS setup

The study analyzes the machinability of GG25 gray cast iron using the Finite Element Analysis of ANSYS. The block, cutting tool, and cutting insert samples are designed and modeled in SOLIDWORKS. Structural analysis is done by using the ANSYS Workbench in Figure 14.

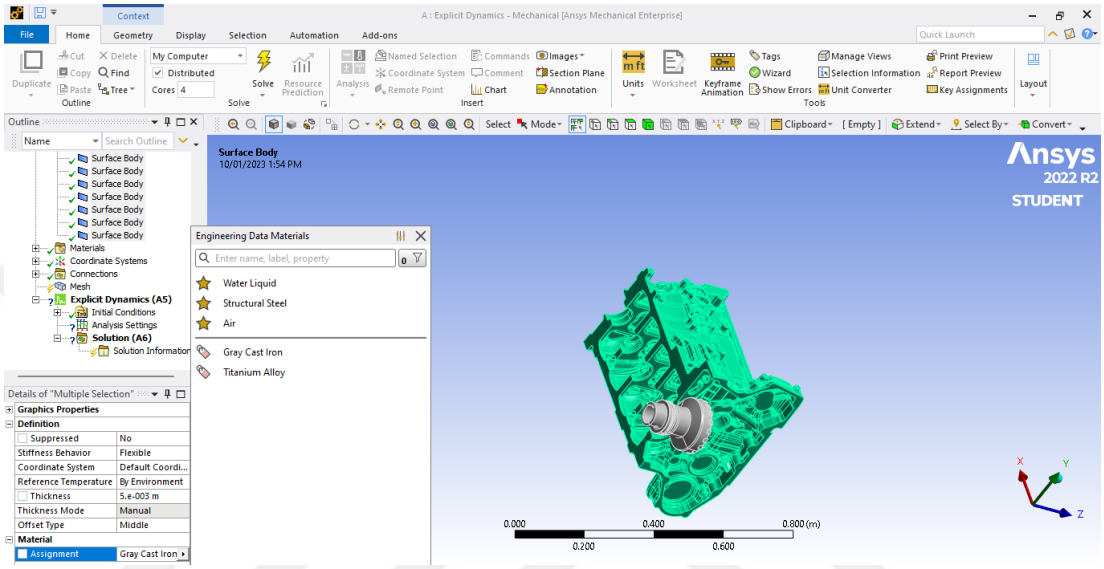

Figure 14: Material selection in ANSYS

While generating mesh properties has been selected as span angle center fine, element order fine, surface mesher program controlled, definition type element size 1 mm seen in Figure 15. Number of nodes found as 4829103 and number of elements was 27661472.

Scope	
Scoping Method	Geometry Selection
Geometry	2 Bodies
Definition	
Suppressed	No
Type	Element Size
Element Size	1.0 mm
Advanced	
Defeature Size	Default
Behavior	Soft
Statistics	
Nodes	4829103
Elements	27661472

Figure 15: Mesh details

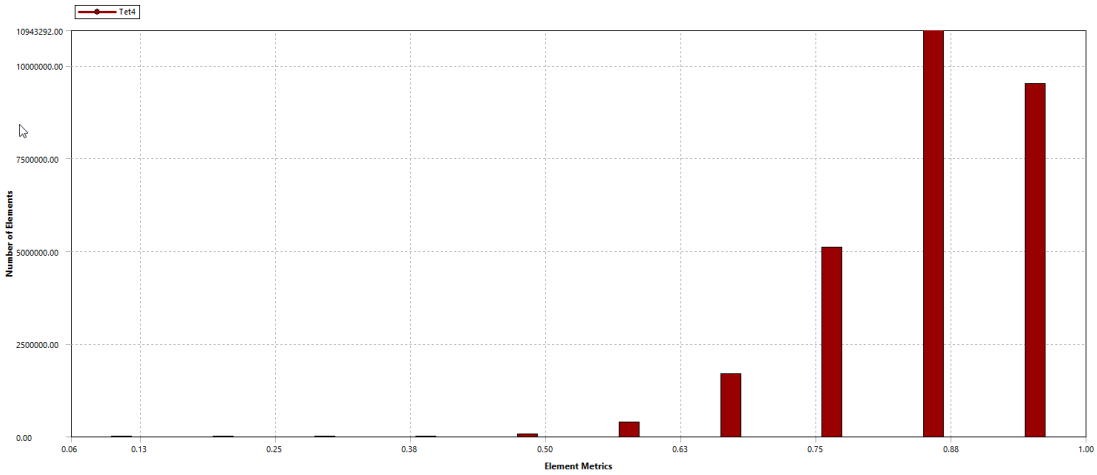

Figure 16: Element quality of mesh metric

Figure 16 shows the result of Element quality of mesh metric. The graph shows that the mesh quality gives high results with 86%, which is the most common area of congestion. Also, other all graphics like orthogonal quality have same consequence with element quality results seen in Figure 17.

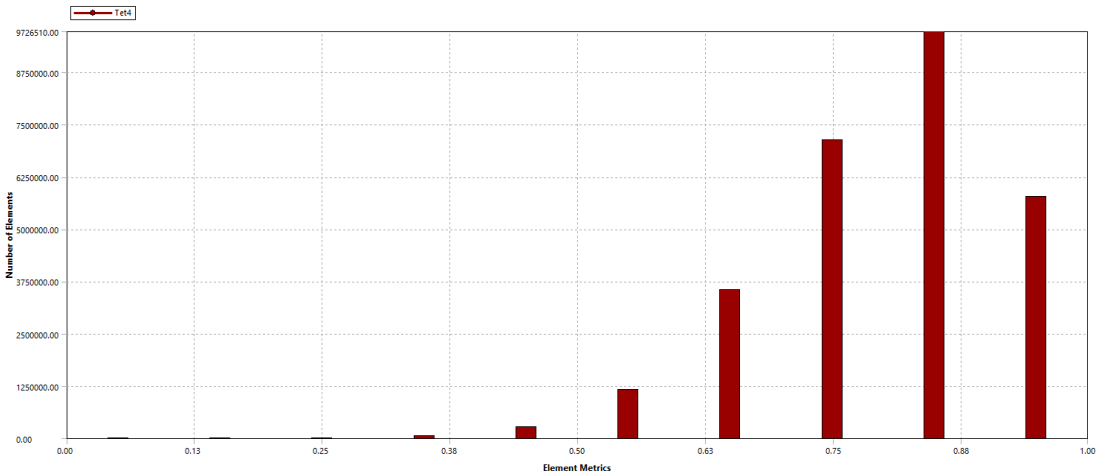

Figure 17: Orthogonal quality of mesh metric

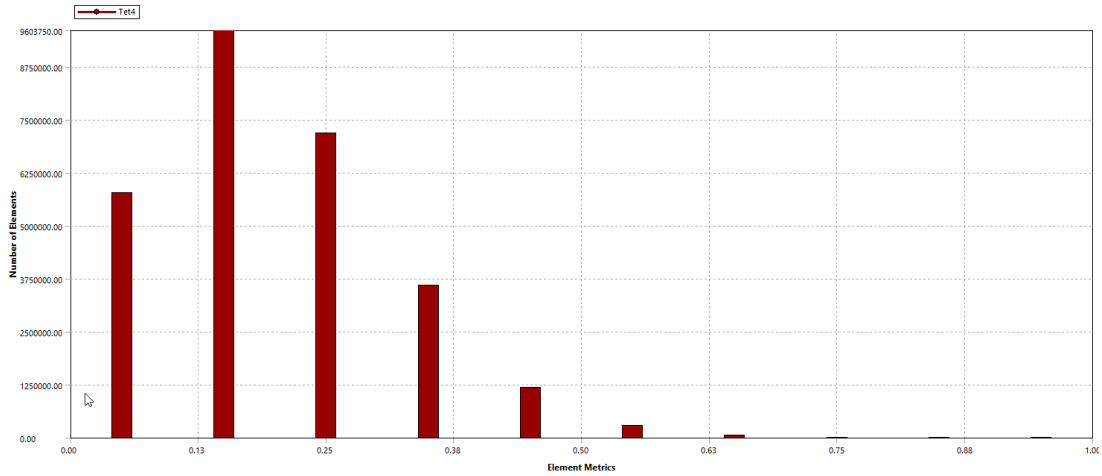

Figure 18: Skewness of mesh metric

In Figure 18 shows result of skewness most congestion area was found 0.15. Within the Ansys software, the metric of skewness is employed as a means to assess the quality of finite element meshes. A finite element mesh refers to a discretized depiction of a geometric structure employed in the context of finite element analysis (FEA) simulations. Skewness pertains specifically to the configuration and deformation of individual components within the mesh.

The measurement of skewness is frequently conducted using a dimensionless metric referred to as the "skewness angle" or "skew angle." The metric is computed for every element within the mesh and quantifies the extent to which an element deviates from an ideal, geometrically well-formed element (typically an equilateral triangle in two dimensions or a regular tetrahedron in three dimensions).

The skewness angle in 2D meshes, specifically triangular elements, is characterized as the largest angle formed by the intersection of the bisectors of the angles within a triangular element. In an ideal scenario, the skewness angle of a perfectly equilateral triangle is zero. The skewness angle in 3D meshes, specifically tetrahedral elements, is determined by evaluating the ratio between the maximum and minimum face angles within the tetrahedron. In the case of a regular tetrahedron, the skewness angle is determined to be zero.

In both scenarios, elevated skewness angles are indicative of increased distortion and deterioration in the quality of the elements. This can result in inaccuracies in the finite element analysis (FEA) outcomes and potentially impact the convergence and stability of the simulation. In general, a mesh of superior quality is characterized by having low skewness values. Nevertheless, the acceptable range of skewness can differ based on the type of analysis and the specific requirements of the simulation.

The Ansys software provides users with the capability to utilize the integrated mesh quality assessment tools for the purpose of evaluating the skewness and other relevant metrics pertaining to their finite element mesh. These software applications enable users to detect and enhance poorly formed components within a mesh structure, thereby enhancing the overall quality of the mesh. This, in turn, contributes to the production of more dependable and accurate simulation outcomes.

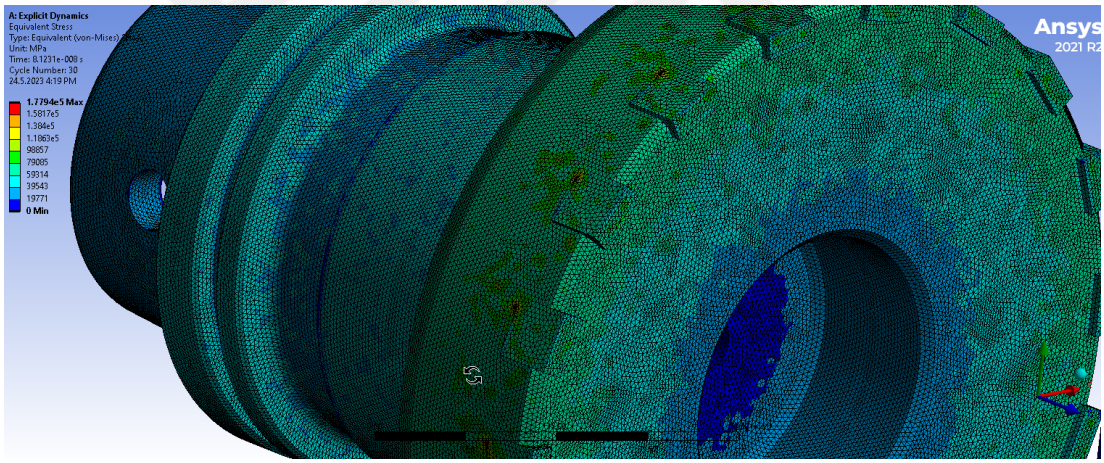

Figure 19: Equivalent stress from ANSYS results

According to ANSYS results, the largest load on the tool is observed at the insert attachment points. A minimum stress value of 19771 MPa and a maximum stress value of 1.78e5 MPa were noted as equivalent stress values seen in Figure 19.

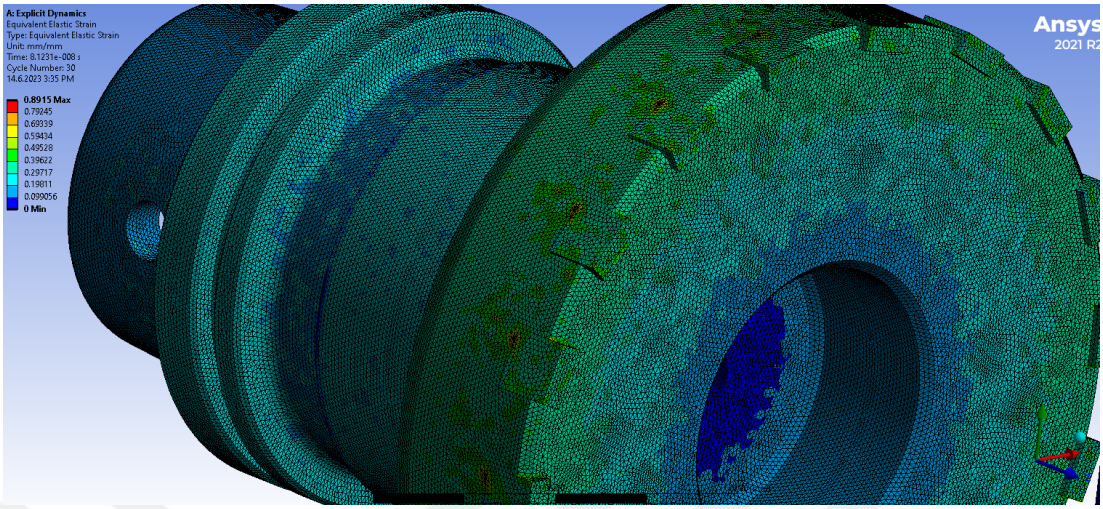

Figure 20: Equivalent strain from ANSYS results

Minimum and maximum values for equivalent elastic strain were found to be 0.099 mm/mm and 0.89 mm/mm, respectively seen in Figure 20.

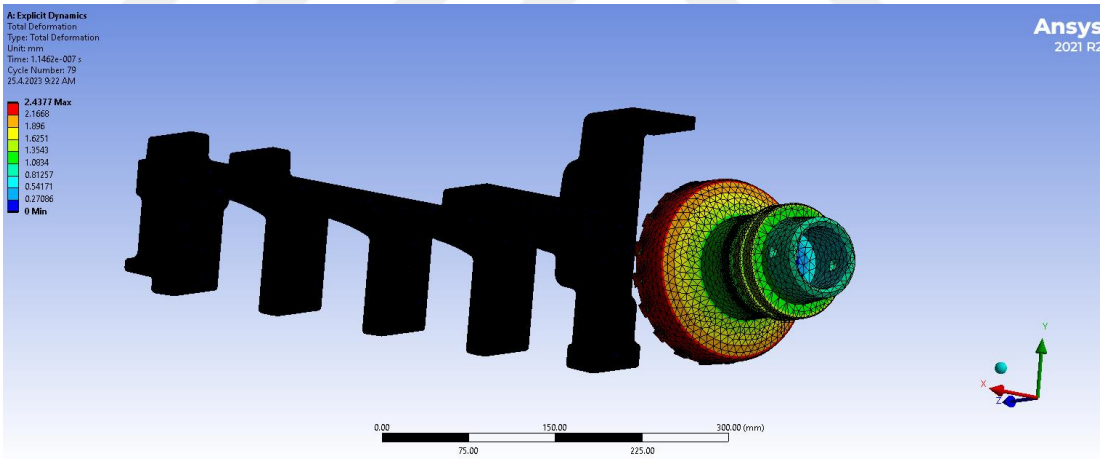

Figure 21: Total deformation from ANSYS results

Total deformation values were observed as a minimum of 0.271 mm and a maximum of 2.438 mm seen in Figure 21.

4.2. Experimental Results

Utilizing coated carbide inserts, 20 HRC GG25 gray cast iron was machined. Figure 22 illustrates an experimental setup in Figure 18 for machining GG25 gray cast iron. Following the measurements of surface roughness, cutting forces, and power consumption, experimental data were analyzed to determine the impact and contribution of the given cutting parameters utilizing RSM, ANOVA, and regression analysis.

Numerous machining experiments were conducted, including various cutting parameters such as cutting speed, feed rate, and depth of cut. The machinability of GG25 gray cast iron was studied through the utilization of various cutting tools featuring different geometries and coatings. The precision machining setup was utilized to conduct experiments, wherein careful measurements were performed to evaluate the quality of the machined surface, cutting forces, and chip morphology.

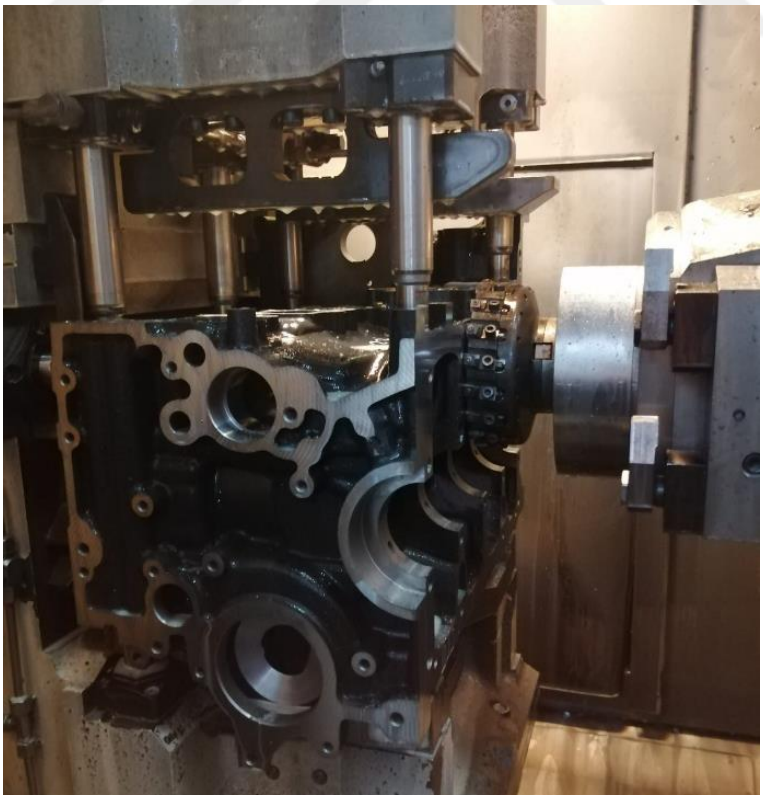

Figure 22: Experimental setup

The experimental results for cutting force, power consumption, and surface roughness for various combinations of machining parameters as determined by Taguchi design. The cutting force was in the range of (14-262) N, the power consumption was in the range of (1116-4115) W, and the surface roughness was in the range of (1.287-4.27) µm, as shown in Table 6.

Table 6: Inputs and outputs of the experimental study

Trial	V_c (m/min)	f (mm/min)	a_p (mm)	R_a (µm)	Force (N)	Power (W)
1	300	2000	0.10	1.49	14	1116
2	300	3000	0.10	2.42	90	1860
3	300	4000	0.10	3.07	112	2149
4	500	2000	0.10	1.45	15	1866
5	500	3000	0.10	2.40	106	2544
6	500	4000	0.10	3.04	115	2664
7	700	2000	0.10	1.29	18	1997
8	700	3000	0.10	2.22	124	2129
9	700	4000	0.10	2.93	132	2817
10	300	2000	0.30	1.98	81	2048
11	300	3000	0.30	2.57	139	2245
12	300	4000	0.30	3.44	144	2958
13	500	2000	0.30	1.72	84	2132
14	500	3000	0.30	2.51	165	2418
15	500	4000	0.30	3.22	178	2992
16	700	2000	0.30	1.62	85	2379
17	700	3000	0.30	2.45	174	3098
18	700	4000	0.30	3.09	180	3163
19	300	2000	0.50	2.18	194	2154
20	300	3000	0.50	2.68	213	3537
21	300	4000	0.50	4.27	198	3320
22	500	2000	0.50	2.12	195	2467
23	500	3000	0.50	2.65	224	3537
24	500	4000	0.50	3.51	249	4023
25	700	2000	0.50	2.07	225	3569
26	700	3000	0.50	2.58	231	3823
27	700	4000	0.50	3.44	262	4115

4.2.1. Main Effect Plots

To show the impacts of the cutting parameters on the surface roughness, cutting force, and power consumption, the main effect plots are provided in Figures 23 to 25. These figures show that the feed rate has the greatest impact on surface roughness, while the depth of cut is the second influential factor on the R_a. However, cutting speed have negligible effects. Feed rate is the most effective factor on surface roughness due to the impact of $f^{2,}$ as seen in equation 2. The development of feed rate on surface roughness is that higher feed rates generally result in rougher surfaces, while lower feed rates tend to produce smoother surfaces. When the feed rate is increased, the tool engages with the workpiece at a faster rate, leading to more aggressive cutting action. This can cause greater tool vibrations, increased friction, and larger chip formation, which can result in a rougher surface finish. Conversely, reducing the feed rate allows for more controlled cutting, minimizing vibrations and promoting smaller chip formation, leading to a smoother surface finish. However, it's important to note that the relationship between feed rate and surface roughness can also depend on various factors, such as the cutting tool, workpiece material, and machining conditions. As a result, using a combination of a low feed rate and a fast cutting speed produces the optimum surface quality [36].

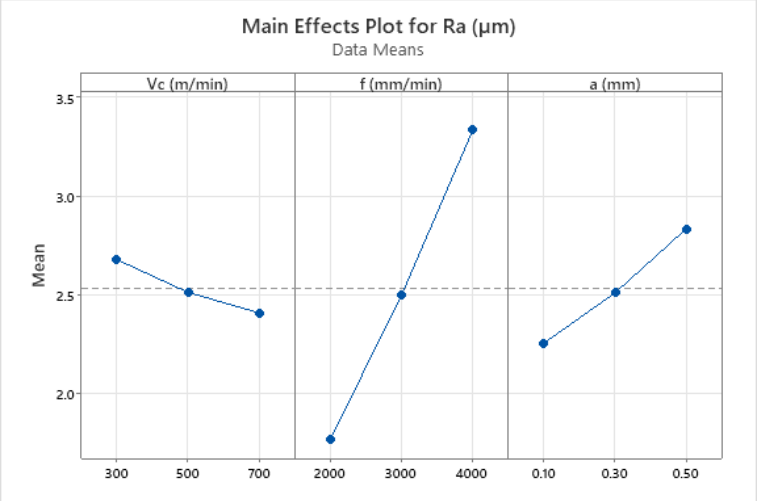

Figure 23: Main effects plot for surface roughness (R_a)

The same results happen for cutting force and power consumption. Increasing the depth of the cut increases the cutting force and power consumption value. Depth of cut is the most influential factor for cutting force and power consumption since it removes deeper removal of chips from the part. The effect of depth of cut on cutting force is that increasing the depth of cut generally leads to higher cutting forces. The depth of cut refers to the distance between the original and final surface of the workpiece that is removed during the cutting process. When the depth of cut is increased, more material is removed in each pass, which requires the cutting tool to exert greater cutting force to overcome the resistance of the workpiece material. This increased cutting force is necessary to penetrate deeper into the material and sever the chips effectively. Additionally, a larger depth of cut leads to a larger contact area between the cutting tool and the workpiece, resulting in a greater surface area for the cutting forces to act upon. This larger contact area increases the friction and interaction between the tool and workpiece, requiring more cutting force to maintain the cutting action. It's important to note that the relationship between the depth of cut and cutting force can be influenced by various factors, such as the cutting tool geometry, cutting speed, workpiece material properties, and machining conditions [37].

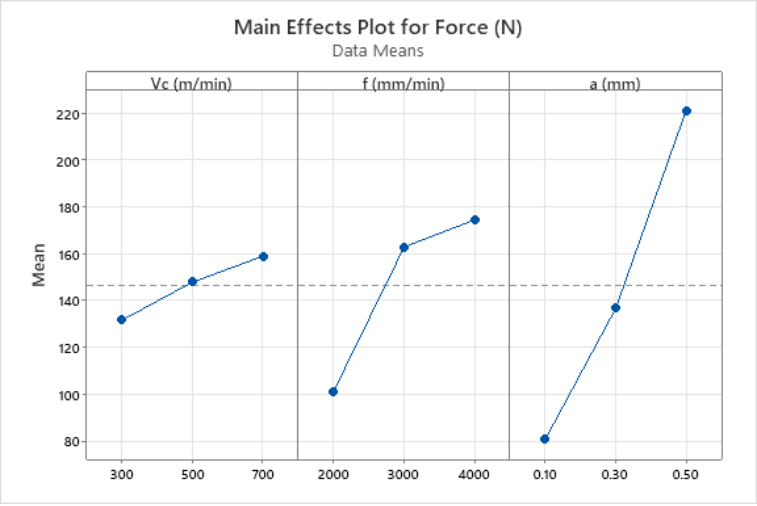

Figure 24: Main effects plot for cutting force (*N*)

Spindle speed has more effect on power consumption than cutting force, as expected. This is due to the fact that higher rotational speeds provide more energy consumption for CNC machines. Power consumption during machining processes can increase as spindle speed, feed rate, and depth of cut increase. Several things may be used to explain this connection. Cutting forces more cuts are performed per unit of time as spindle speed, feed rate, and depth of cut increase because the cutting tool contacts with the workpiece more frequently. Together, these characteristics result in greater cutting forces, which need more power to overcome resistance observed during cutting. Increased spindle speed, feed rate, and depth of cut all have an impact on how much friction there is between the cutting tool and the workpiece. The frictional losses develop with greater contact areas and higher relative velocities between the surfaces. In order to counteract and overcome these frictional forces and provide steady machining processes, additional power consumption is thus required. In summary, increased cutting pressures intensified frictional effects, the requirement for managing larger material removal rates, and the influence of tool wear are the main causes of the increase in power consumption as spindle speed, feed rate, and depth of cut increase. Understanding these components is essential for managing production costs, improving energy efficiency, and optimizing machining processes in manufacturing operations [38].

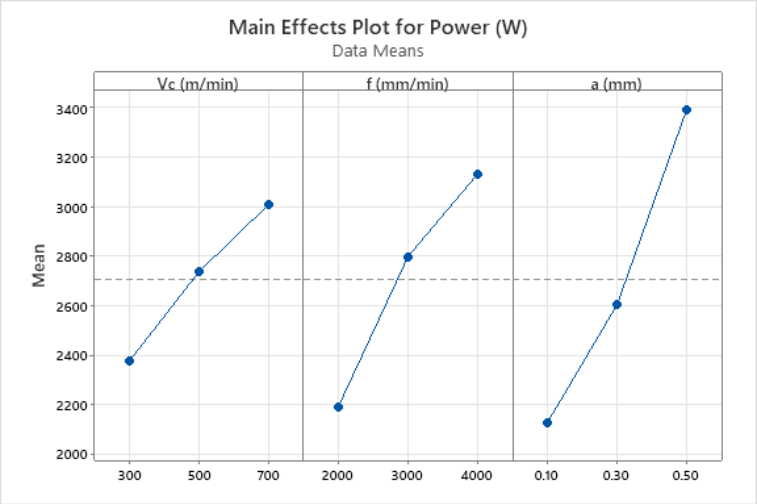

Figure 25: Main effects plot for power consumption (*W*)

4.2.2. Analysis of Variance (ANOVA)

In this study, the MiniTAB software was utilized to apply ANOVA to determine the statistical significance of the feed rate, the cutting speed, and the depth of cut on the surface roughness, cutting force, and power consumption. In addition, the regression equations were developed to predict the output factors without doing any experiments.

The most important machining factors that affect surface roughness were determined by analyzing the variance, as shown in Table 7. P is the significant factor, D is the degree of freedom, and F is the variance ratio in this table. The importance level alpha used for this investigation was 0.05. When the P-value is less than 0.05, the influence of the input parameter on the response variable is significant. The ANOVA results for surface roughness, cutting force, and power consumption are given in Tables 7 to 9. According to this table, the feed rate (f), which accounts for 82.37% of the variation, is the crucial factor in surface roughness. The depth of cut (a_p) contribution to (R_a) is 11.15%, which also has a minor effect. There is a minor effect of cutting speed on surface roughness.

Table 7: ANOVA results for surface roughness

Source	DF	Seq SS	Adj SS	Adj MS	F-Value	P-Value	Contribution
Model	9	12.9536	12.9536	1.4393	53.27	0.000	96.58%
Linear	3	12.8682	12.8682	4.2894	158.77	0.000	95.94%
V_c	1	0.3248	0.3248	0.3248	12.02	0.003	2.42%
f	1	11.0481	11.0481	11.0481	408.94	0.000	82.37%
a_p	1	1.4953	1.4953	1.4953	55.35	0.000	11.15%
Square	3	0.0297	0.0297	0.0099	0.37	0.779	0.22%
$V_c \times V_c$	1	0.0057	0.0057	0.0057	0.21	0.652	0.04%
$f \times f$	1	0.0167	0.0167	0.0167	0.62	0.442	0.12%
$a_p \times a_p$	1	0.0073	0.0073	0.0073	0.27	0.611	0.05%
2-Way Interaction	3	0.0557	0.0557	0.0186	0.69	0.572	0.42%
$V_c \times f$	1	0.0352	0.0352	0.0352	1.30	0.269	0.26%
$V_c \times a_p$	1	0.0204	0.0204	0.0204	0.76	0.397	0.15%
$f \times a_p$	1	0.0001	0.0001	0.0001	0.00	0.949	0.00%
Error	17	0.4593	0.4593	0.0270			3.42%
Total	26	13.4129					100.00%

Table 8 shows the ANOVA results for cutting force. It is clear that, with a contribution of 68.82%, the depth of cut is the primary factor affecting cutting force. With a contribution of 18.68%, the feed rate also significantly affects the cutting force. However, cutting speed and the interaction of $f \times a$ and $f \times f$ has a negligible influence on the response.

Table 8: ANOVA results for cutting force

Source	**DF**	**Seq SS**	**Adj SS**	**Adj MS**	**F-Value**	**P-Value**	**Contribution**
Model	9	126142	126142	14015.8	78.38	0.000	97.65%
Linear	3	116390	116390	38796.7	216.95	0.000	90.10%
V_c	1	3362	3362	3362.0	18.80	0.000	2.60%
f	1	24127	24127	24126.7	134.92	0.000	18.68%
a_p	1	88901	88901	88901.4	497.14	0.000	68.82%
Square	3	5029	5029	1676.3	9.37	0.001	3.89%
$V_c \times V_c$	1	39	39	39.2	0.22	0.646	0.03%
$f \times f$	1	3767	3767	3766.7	21.06	0.000	2.92%
$a_p \times a_p$	1	1223	1223	1223.1	6.84	0.018	0.95%
2-Way Interaction	3	4723	4723	1574.3	8.80	0.001	3.66%
$V_c \times f$	1	547	547	546.7	3.06	0.098	0.42%
$V_c \times a_p$	1	252	252	252.1	1.41	0.251	0.20%
$f \times a_p$	1	3924	3924	3924.1	21.94	0.000	3.04%
Error	17	3040	3040	178.8			2.35%
Total	26	129182					100.00%

The ANOVA result for power consumption is given in Table 9. According to the findings, depth of cut (a_p) dominates power consumption with a 49.34% contribution. It was followed by feed rate and cutting speed with a 27.24% and 12.34% contribution, respectively. Therefore, all cutting parameters are effective on the power consumption.

Table 9: ANOVA results for power consumption

Source	DF	Seq SS	Adj SS	Adj MS	F-Value	P-Value	Contribution
Model	9	13436723	13436723	1492969	21.09	0.000	91.78%
Linear	3	13019130	13019130	4339710	61.30	0.000	88.93%
V_c	1	1806901	1806901	1806901	25.52	0.000	12.34%
f	1	3988429	3988429	3988429	56.33	0.000	27.24%
a_p	1	7223801	7223800	7223800	102.03	0.000	49.34%
Square	3	270921	270921	90307	1.28	0.314	1.85%
$V_c \times V_c$	1	12120	12120	12120	0.17	0.684	0.08%
$f \times f$	1	111430	111430	111430	1.57	0.227	0.76%
$a_p \times a_p$	1	147371	147371	147371	2.08	0.167	1.01%
2-Way Interaction	3	146671	146671	48890	0.69	0.570	1.00%
$V_c \times f$	1	76640	76640	76640	1.08	0.313	0.52%
$V_c \times a_p$	1	38307	38307	38307	0.54	0.472	0.26%
$f \times a_p$	1	31724	31724	31724	0.45	0.512	0.22%
Error	17	1203575	1203575	70799			8.22%
Total	26	14640297					100.00%

4.2.3. 3D Surface Plots for Cutting Parameters

The ANOVA results show how cutting parameters affect surface roughness, cutting force, and power consumption values. The feed rate is the most crucial cutting parameter for surface roughness, whereas the depth of cut matters for cutting force and power consumption. Surface roughness values are sharply enlarged when the feed rate rises, and it rises by increasing the depth of cut, while it drops by increasing the cutting speed. The 3D graph related to the effect of cutting parameters on surface roughness, cutting force, and power consumption for carbide inserts is depicted in Figures 26, 27, and 28, respectively.

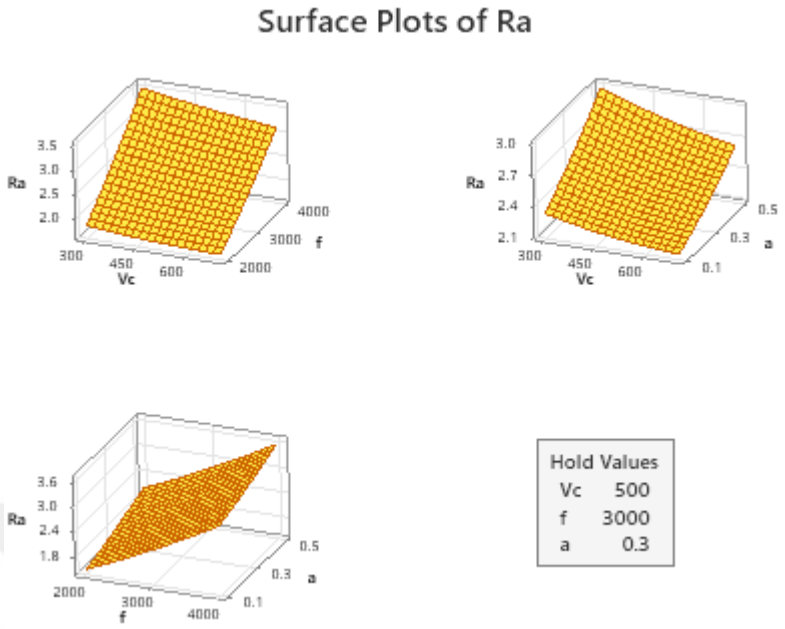

Figure 26: Effects of cutting parameters on surface roughness

The cutting parameters used during machining operations, including spindle speed, feed rate, and depth of cut, have essential effects on the resultant cutting forces. The previously mentioned variables have a direct impact on the cutting force and features of the cutting forces faced while performing the cutting operation. Understanding these effects is essential in achieving effective and accurate machining. The reduction of cutting parameters has significant effects on cutting forces [39].

1. Spindle Speed

- The increase in spindle speed results in an increase in cutting forces.
- Increased spindle speeds produce a higher rate of tool engagement with the workpiece, which results in an increased number of cuts per unit of time.
- The increased frequency of cutting increases cutting forces due to the requirement to remove material in less time.
- The higher cutting forces can be influenced by factors such as tool geometry, material properties, and specific cutting parameters.

2. Feed Rate

- An increase in feed rate frequently results in more cutting forces.
- Higher feed rates result in more contact between the cutting tool and the workpiece, which increases the frictional forces and, as a result, the cutting forces.

3. Depth of Cut

- Increase in the cut depth results in an expansion in the cutting forces.
- The removal of a greater quantity of material in each pass is directly related to the depth of the cut. This is because deeper cuts typically result in larger contact areas between the tool and the workpiece, which consequently leads to an increase in frictional forces and, subsequently, higher cutting forces.

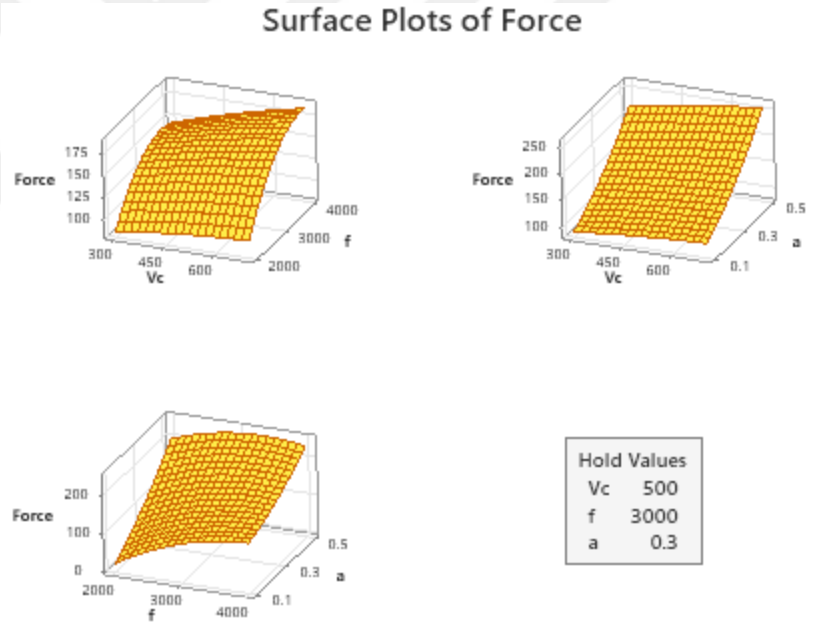

Figure 27: Effects of cutting parameters on cutting force

The amount of material removed in each pass directly depends on the depth of the cut. Higher cutting forces are produced as the depth of cut rises because more material is sheared and displaced. The chip's cross-sectional area increases with the depth of the cut, and the cutting force is proportional to this increment. Higher cutting forces put additional strain on the workpiece, the machine, and the cutting tool.

Cutting forces directly affect how much power consumption is used during CNC milling. More power consumption is needed to push the tool through the material at higher cutting forces. As the cutting forces rise, so does the power consumption of the spindle motor, feed drives, and auxiliary systems. Consequently, deeper cuts often result in higher power consumption needs [40].

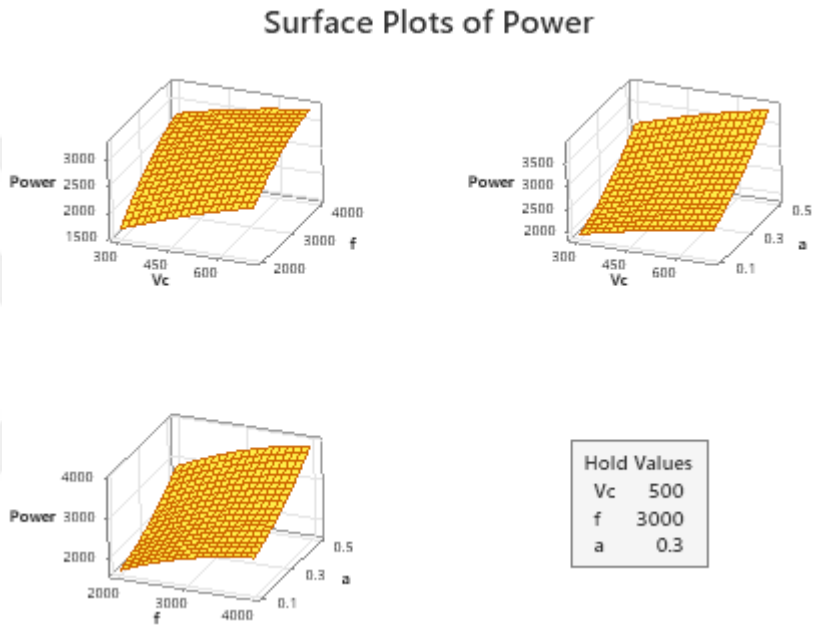

Figure 28: Effects of cutting parameters on power consumption

It is essential to recognize that the effect of cutting parameters on cutting forces may demonstrate variability dependent on factors such as the material of the workpiece, tool geometry, cutting tool material, cutting conditions, and the specific machining operation. Moreover, cutting forces may be subject to various factors, such as tool deflection and using coolant or lubrication.

By understanding the effect of cutting parameters on cutting forces, manufacturers and machinists can optimize indicated parameters to achieve the desired cutting forces, reduce power consumption, and ensure efficient and accurate machining processes [41].

4.2.4. Contour Plots for Responses

According to the contour plot presented in Figure 29, higher spindle speed and lower feed rate leads to the minimum surface roughness. Moreover, the interaction of cutting speed and depth of cut reveals that low a_p and high V_c result in minimum R_a. Finally, when the $a_p \times f$ graph is examined, it is observed that low depth of cut and feed rate values lead to quite optimum results for surface roughness. The results from all graphs show that f has the most significant effect, and V_c has the smallest effect on R_a.

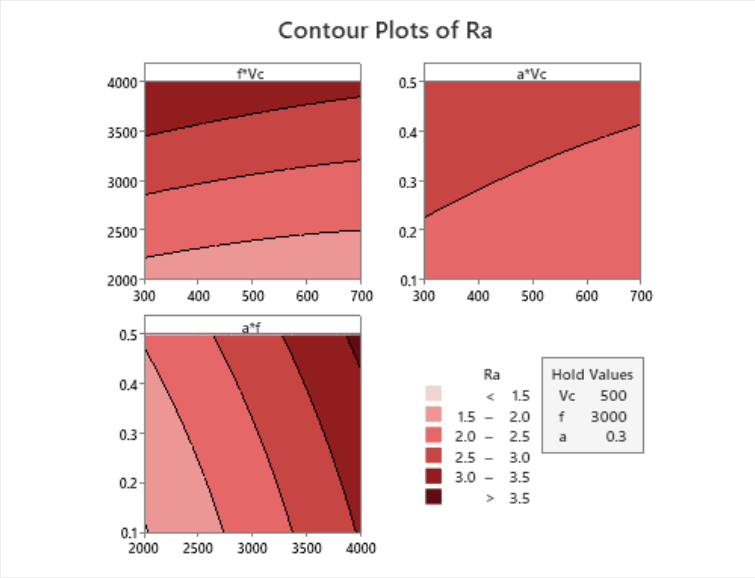

Figure 29: Contour plot of surface roughness

According to the contour plot presented in Figure 30, lower spindle speed and lower feed rate give optimal results for cutting force. In addition, the lower cutting force is obtained with a combination of the least depth of cut and spindle speed. Lastly, when the $a_p \times f$ graph is examined, it is observed that low depth of cut and feed rate values lead to minimum results for cutting force. When all the graphs are examined, it is clear that the value of ap has the greatest effect, and the value *Vc* has the smallest effect on cutting force.

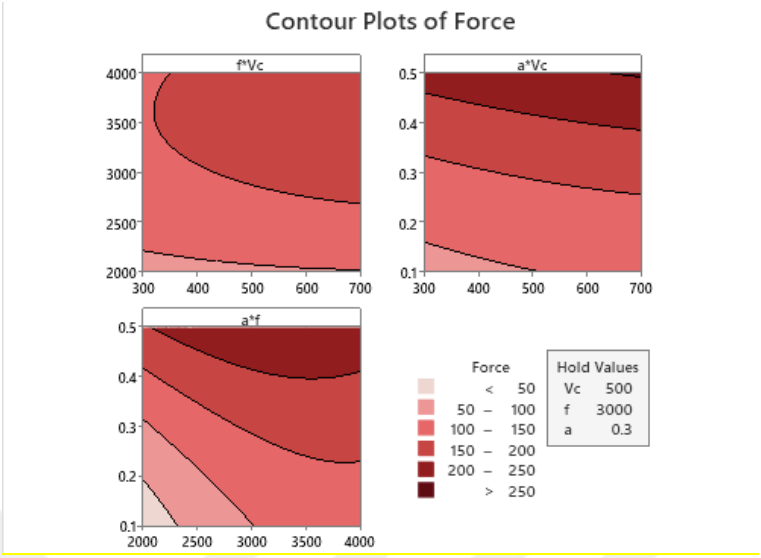

Figure 30: Contour plot of cutting force

According to the contour plot for the power consumption in Figure 31, lower spindle speed and lower feed rate situation give the optimal results for power consumption. Second graph clearly states that the best results for power consumption are examined when the depth of cut value and spindle speed value are low. Lastly, when the $a_p \times f$ graph is examined, it is observed that low depth of cut and feed rate values lead to quite optimum results for power consumption. When all the graphs are examined, it is clear that a value has the greatest effect and value V_c has the smallest effect.

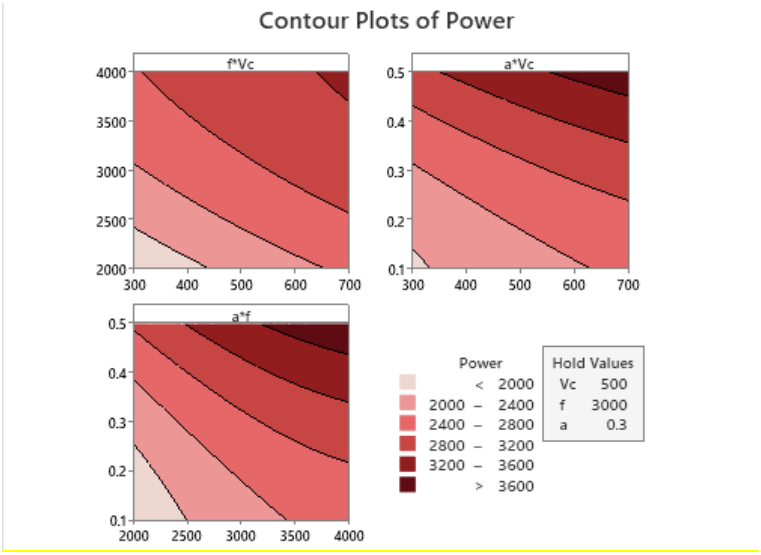

Figure 31: Contour plot of power consumption

4.2.5. Examination of Standardized Effects with Normal Plot

In order to better understand the data, the normal probability plot is generated by plotting the arranged data alongside an approximation of the means or medians of the corresponding order statistics. A normal probability plot is used to identify whether a tiny data collection originates from a normal distribution. In other terms, the process is normally distributed if the diagram yields a straight line. In this examination, α used as 0.005.

Figure 32 shows the normal plot of the standardized effects for surface roughness. The parameters that are located on the right side of the straight line have a direct effect, while the parameters on the left side have an indirect effect. It has been observed that the most effective factor for surface roughness is feed rate. The next important parameter is the depth of cut. It was followed by cutting speed with an inverse effect. Other parameters do not have a significant factor effect on R_a.

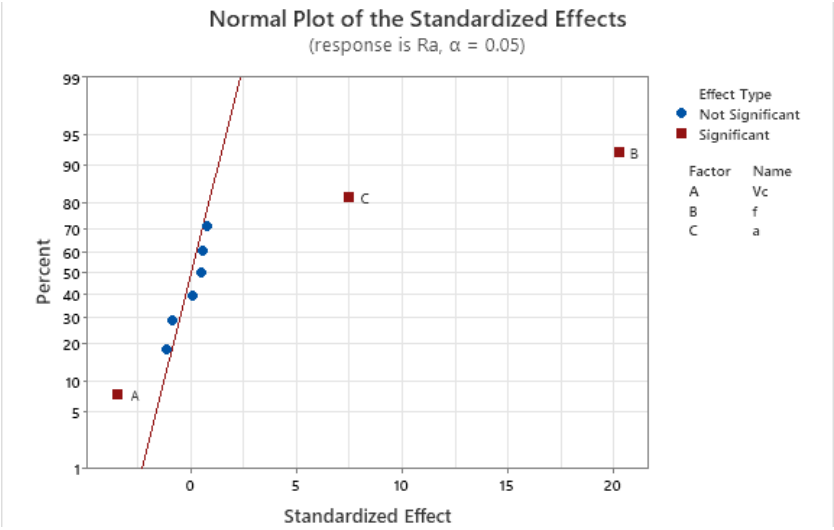

Figure 32: Normal plot of surface roughness

The normal plot of the normalized effects for cutting force is in Figure 33. The depth of cut has been found to have the greatest impact on cutting force. The feed rate is the following critical variable. Cutting speed and square of the depth of cut came after. However, cutting force is indirectly influenced by the feed rate square and the feed rate depth of cut interaction. Other factors have a negligible impact on cutting force.

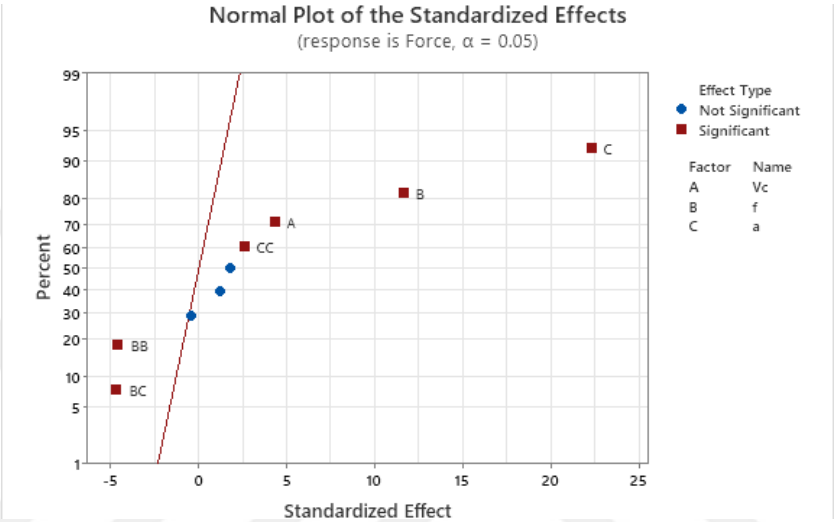

Figure 33: Normal plot of cutting force

Similar to cutting force, the depth of cut is the most effective factor for power consumption in Figure 34. Feed rate is the next important parameter. Cutting speed came after the feed. The impact of other variables on power consumption is negligible.

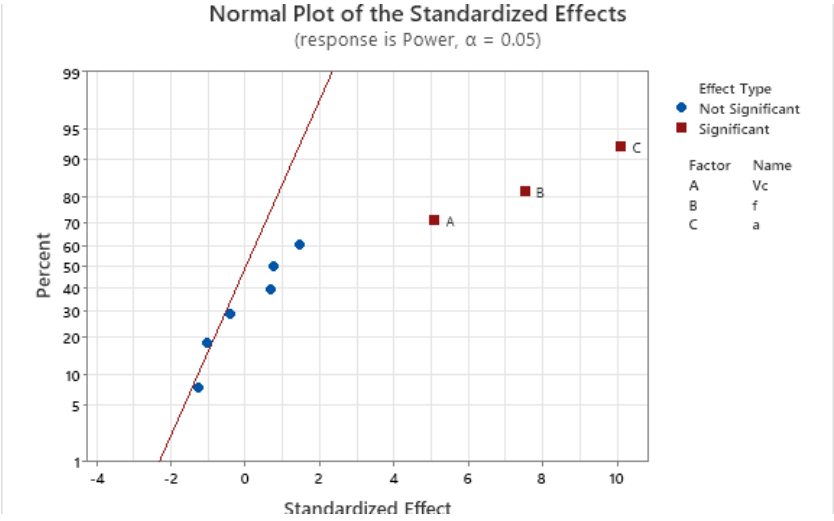

Figure 34: Normal plot of power consumption

4.2.6. Regression Equations

To determine the relationship between the dependent and independent variables, regression models were developed. In order to suggest the optimal equation, the determination coefficient (R^2) is computed for the dependent variables.

This research developed quantitative models using input variables like cutting speed, feed rate, and depth of cut during the milling of GG25 gray cast iron. To evaluate experimental data and develop an optimization model for responses, MiniTAB software was used. The developed equation for predicting the surface roughness, cutting force, and power consumption is given in Equations (3), (4), and (5), respectively.

Regression Equation for Surface Roughness

$$R_a = 0.206 - 0.00032\ V_c + 0.000598\ f + 1.39\ a_p + 0.000001\ V_c \times V_c + 0.000000\ f \times f + 0.87\ a_p \times a_p - 0.000000\ V_c \times f - 0.00103\ V_c \times a_p + 0.000015\ f \times a_p \quad (3)$$

Model Summary

R-sq	R-sq(adj)
96.58%	94.76%

Regression Equation for Cutting Force

$$\text{Force} = -317.3 - 0.003\ V_c + 0.1972\ f + 351\ a_p - 0.000064\ V_c \times V_c - 0.000025\ f \times f + 357\ a_p \times a_p + 0.000034\ V_c \times f + 0.1146\ V_c \times a_p - 0.0904\ f \times a_p \quad (4)$$

Model Summary

R-sq	R-sq(adj)
97.65%	94.40%

Regression Equation for Power Consumption

$$\text{Power} = -1741 + 3.48\,V_c + 1.411\,f - 661\,a_p - 0.00112\,V_c \times V_c - 0.000136\,f \times f + 3918\,a_p \times a_p - 0.000400\,V_c \times f + 1.41\,V_c \times a_p + 0.257\,f \times a_p \quad (5)$$

Model Summary

R-sq	R-sq(adj)
91.78%	87.43%

4.2.7. Optimization of Cutting Parameter

In a manufacturing process with several variables, determining the ideal cutting parameters is particularly difficult by computing the mean of each response parameter in relation to each input parameter. So, the tables below from 10 to 12 show the cutting parameters corresponding to the lowest values.

Table 10: Optimization of cutting parameters

Response	Goal	Lower	Target	Upper	Weight	Importance
Power	Minimum	1116,00	4115,00		1	1
Force	Minimum	14,00	262,00		1	1
R_a	Minimum	1,29	4,27		1	1

Table 11: Optimization of cutting parameter solutions

Solution	V_c	f	a_p	Power Fit	Force Fit	Ra Fit	Composite Desirability
1	300	2000	0,100000	1306,93	14,4352	1,54319	0,948908
2	300	2000	0,104295	1311,55	15,6278	1,54872	0,946220
3	300	2000	0,106464	1313,95	16,2348	1,55152	0,944848
4	300	2000	0,190421	1434,87	42,3197	1,66641	0,884056
5	300	2000	0,205947	1463,28	47,6951	1,68900	0,871141

The machinability of GG25 gray cast iron was improved by determining the optimal cutting parameters through empirical testing and analysis that followed. Suggestions were given to optimize productivity, improve surface quality, and increase tool lifespan by modifying cutting speed, feed rate, and depth of cut.

The study's show for optimized cutting parameters holds practical implications for industries that participated in machining GG25 gray cast iron. The addition of these parameters has the potential to result in improved efficiency, better surface finish, and decreased tooling costs. Manufacturers can use the results of the study to optimize their machining procedures and improve the competitiveness of their company's operations.

Table 12: Multiple response prediction

Variable	**Setting**
V_c	300
f	2000
a_p	0,1

Response	**Fit**	**SE Fit**	**95% CI**	**95% PI**
Power	1307	190	(906; 1708)	(617; 1997)
Force	14,44	9,54	(-5,70; 34,57)	(-20,23; 49,10)
R_a	1,543	0,117	(1,296; 1,791)	(1,117; 1,969)

The ANOVA analysis revealed that feed rate is the factor that has the greatest impact on surface roughness. Due to the creation of a continuous chip that raises the temperature of both the workpiece and the tool, high feed rates and high depth of cut have a negative impact on surface quality. The high cutting force increases tool to workpiece friction, which increases surface roughness. The same procedure applies to power consumption. Surface roughness, cutting force, and power consumption value increase as the feed rate rises. Additionally, the surface roughness is reduced at greater cutting speeds. As a result, using a combination of a low feed rate and a fast cutting speed produces the optimum surface quality. According to the ANOVA results, depth of cut and feed rate impact surface roughness, cutting force, and power consumption.

The effort of determining optimal cutting parameters in a manufacturing process that involves numerous variables is particularly arduous when dependent on the computation of the mean of each response parameter in relation to each input parameter. Figure 32 displays the cutting parameters that correspond to the minimum values for responses. The optimal cutting parameters, including a cutting speed of 300 m/min, feed rate of 2000 mm/min, and depth of cut of 0.1 mm, can result in the least surface roughness (1.54 µm), cutting force (14.43 N), and power consumption (1306.92 W) during the cutting process seen in Figure 35.

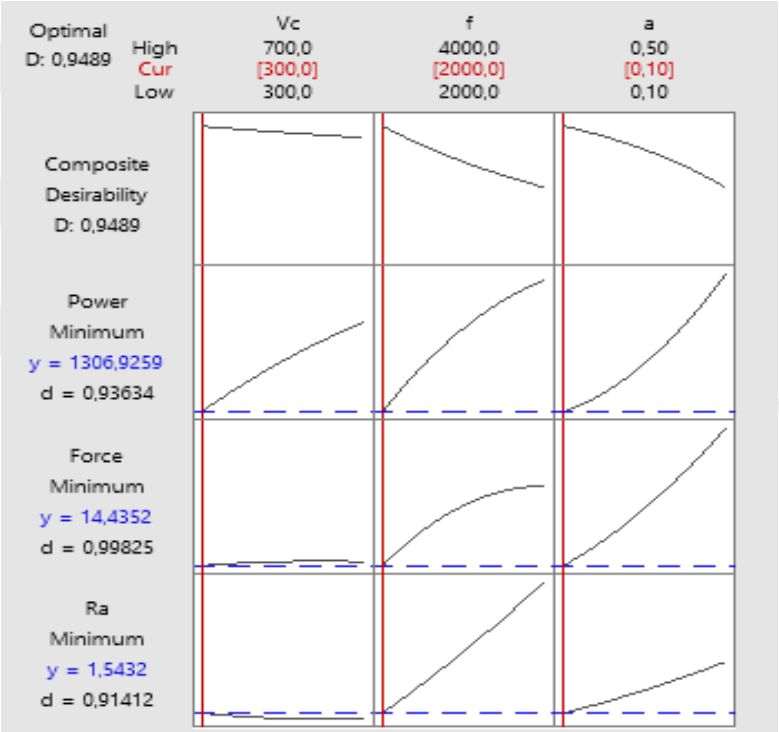

Figure 35: Response optimization: power consumption, cutting force, surface roughness

It's important to understand that the relationship between cutting force, power consumption, and depth of cut is not linear. Other variables also influence these characteristics, including cutting speed, feed rate, and material properties. To balance the intended material removal rate with the machine's power consumption restrictions and tool capabilities, it is essential to optimize the depth of cut together with other cutting parameters [42].

Choosing the right depth of cut is also essential to getting the best machining results. While an extremely large depth of cut can result in problems, including excessive tool wear, poor surface finish, and a greater chance of tool breakage, an excessively small depth of cut may result in longer machining time. Therefore, for effective and profitable CNC milling operations, affecting the ideal balance between productivity, cutting forces, power consumption, and tool life is essential [43].

4.2.8. Confirmation Test

In this experimental study, a confirmation test has been performed on the six random cutting parameters combination in the range of initial cutting parameters. Firstly, six experimental tests have been conducted based on the presented combination in Table 13; secondly, these combinations are used in the developed regression equations, and the experimental and predicted results are compared in Table 14.

According to the findings, the percentage error for each combination of acceptable range. It is particularly challenging to guarantee the correct cutting parameters in manufacturing processes with many moving parts by calculating the mean of each response parameter as suggested by each input parameter.

According to the ANOVA results, the feed rate is the factor that has the biggest impact on surface roughness. High feed rates negatively affect surface quality because they induce a continuous chip to form, raising the temperature of both the tool and the workpiece. The increased surface roughness results from increased friction between the workpiece and the tool caused by high temperature. Consequently, a combination of high cutting speed, low depth of cut, and low feed rate produces the finest surface quality.

Table 13: Cutting parameters combination for the confirmation test

Trial	V_c (m/min)	f (mm/min)	a_p (mm)
1	350	2250	0.15
2	400	2500	0.20
3	450	2750	0.25
4	550	3250	0.35
5	600	3500	0.40
6	650	3750	0.45

Table 14: Comparison of experimental and predicted results

	Predicted			Experimental			Error (%)		
Trial	R_a	**Force**	**Power**	R_a	**Force**	**Power**	R_a	**Force**	**Power**
1	1.74	53.91	1661	1.72	52	1875	1.22%	3.68%	11.42%
2	1.97	90.46	2015	1.98	90	2159	0.46%	0.51%	6.66%
3	2.21	124.51	2370	2.18	124	2418	1.16%	0.41%	1.99%
4	2.69	185.12	3081	2.65	180	3163	1.43%	2.84%	2.60%
5	2.94	211.67	3437	3.04	202	3503	3.42%	4.79%	1.88%
6	3.19	235.74	3794	3.32	267	4155	3.95%	11.71%	8.70%
					Mean Error (%)		**1.94%**	**3.99%**	**5.54%**

The confirmation test serves to validate the surface roughness results obtained from the previous investigation. The confirmation test's Ra values are compared with before empirical results. The present study involves analysis and discussion of any observed differences or similarities to validate the consistency of the findings related to surface roughness see Figure 36.

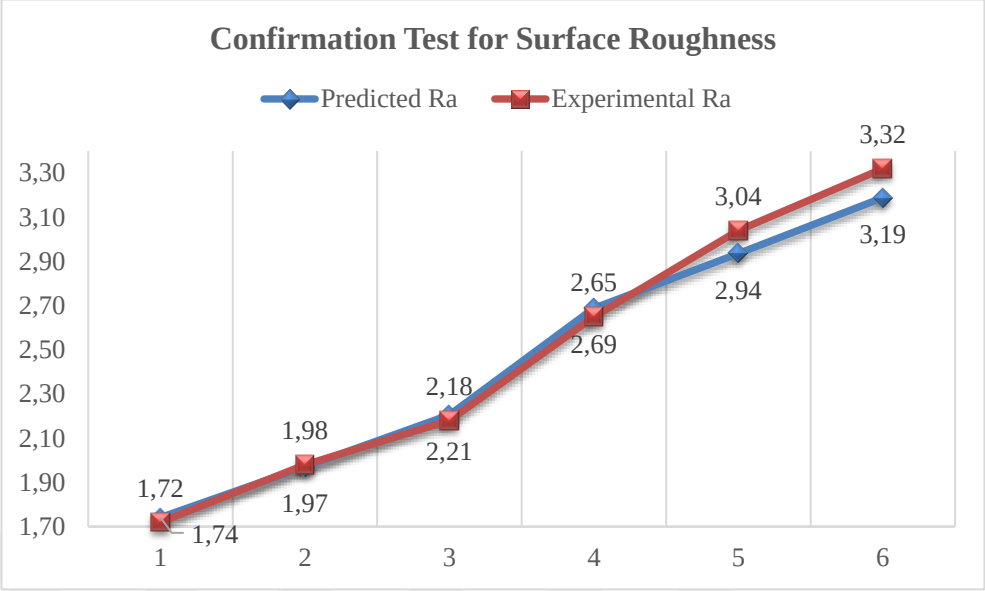

Figure 36: Confirmation test comparison graph for surface roughness

The cutting force measurements obtained from the confirmation test are compared with the previously collected empirical data. The cutting forces acting along the X, Y, and Z axes are evaluated, and any inconsistencies or agreements are analyzed to validate the accuracy and reliability of the previous cutting force results see Figure 37.

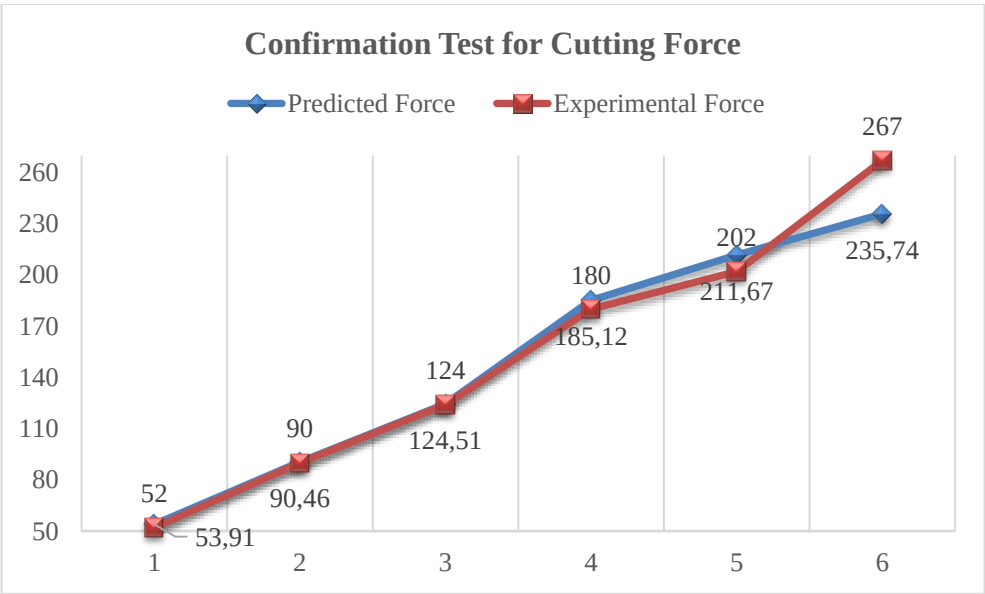

Figure 37: Confirmation test comparison graph for cutting force

The confirmation test's power consumption results are compared with the previous empirical findings. The analysis and discussion of power consumption patterns' variations and similarities are conducted to verify existing empirical results see Figure 38.

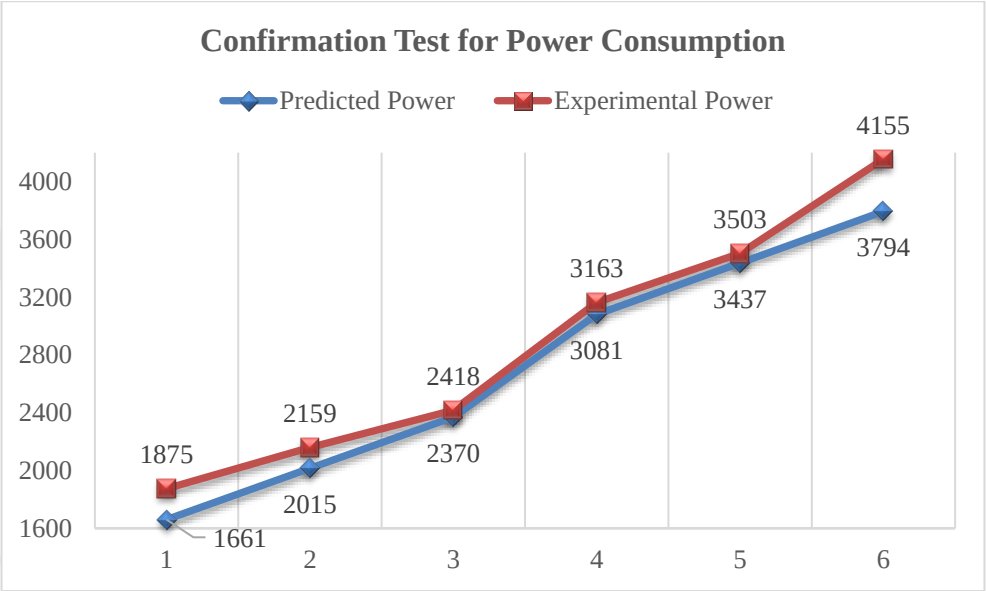

Figure 38: Confirmation test comparison graph for power consumption

According to the surface roughness results, the error percentage was observed between 0.46% and 3.95%, with the best error percentage for cutting force of 0.41%, i.e., less than one percent, and the sixth trial error percentage of 11.71% in the most challenging attempt. This result may vary according to the current environmental conditions or the necessity of the maintenance of the machine. In addition, there were slight differences in the predicted result of 236 Newtons while the experimental result was 267 Newtons. Similarly, power consumption gave an error percentage from 1.88% to 11.42%. In the first trial, it was thought that with 11.42%, it could be affected by conditions in a similar way to cutting force in precision machining. Relevant results have been observed in other trials.

The mean error for the surface roughness is 1.94%. This result shows that the outputs of the prepared regression equation are very accurate. The mean error for cutting force was calculated as 3.99%. A result close to the ANOVA analysis for cutting force was found. For power consumption, it was calculated as 5.54%. This result, the error contribution calculated in the ANOVA analysis for power consumption, remained lower than 8.22%.

4.3. Discussion

The results of the empirical examination replied to important discoveries concerning the machinability of GG25 gray cast iron. The examination of the machined surface quality demonstrated that particular cutting parameters were associated with improved surface finish, whereas others were linked to increased surface roughness. The investigation encompassed an analysis of the relationship between outputs and different cutting parameters.

The study's empirical tests offer significant insights into the machinability of GG25 gray cast iron. The results of this study provide valuable information into the improvement of machining procedures and the identification of suitable tooling approaches for GG25 gray cast iron parts. These findings could improve productivity and financial sustainability in machining activities in important sectors.

In order to evaluate these concepts, an experimental design was implemented in this study to enable the systematic observation of results after a specified number of attempts. This analysis employed three distinct categories of fundamental characteristics, three quantifiable variables, and a singular objective. The investigation was initiated through the establishment of parameters, wherein specific variables were maintained as controlled variables or parameters. Apart from the aforementioned controlled variable, an additional element referred to as a "material parameter" has been duly considered, which accounts for the material's homogeneity and machinability. The parameters of cutting speed (V_c), feed rate (f), and depth of cut (a_p)

are distinct from one another. Subsequently, a consensus was reached to consider three quantifiable variables, namely cutting parameters and center roughness, as the ground-on factors.

The apparatus to be employed in this inquiry has been fabricated and designed exclusively for the purpose of this study. The experiment utilizes a standard material, GG25 (gray cast iron), with dimensions of 540mm in width (horizontal) and 400mm in height (vertical). In contrast to its alternative forms, this particular substance is commonly employed within industrial settings for the purpose of machining. This pig iron can be used in tandem with ceramic or carbide (insert) cutting tools. Carbide-cutting tools offer several advantages, including their exceptional durability and extended lifespan. Carbide is offered in over twelve distinct grades, each with varied applications. Furthermore, it is more cost-effective and efficient. Due to the reasons stated earlier, a cutting tool made of carbide has been utilized for this particular series of experiments. The experimental methodology was meticulously followed, wherein a specialized cutting tool was utilized to cleanse the surface of the CNC Milling Center by 1 mm before proceeding with rough machining to facilitate surface preparation for smoothing.

Encountering liabilities and errors in scientific experiments is a common phenomenon in reality. There are various potential limitations in the experimental design that may have an impact on the results. The experimental methodology utilized in our investigation can be considered devoid of systematic errors, with any observed disparities ascribed to stochastic errors. The statement above is acceptable as the results align with established theories and empirical data.

To sum up, all literature reviews were to gather that the GG25 gray cast iron is a frequently utilized material in various industrial applications. The CNC milling process's machinability of this material can be affected by several factors, including the cutting speed, feed rate, and depth of cut. The machinability of GG25 gray cast iron can be further examined by delving into the impact of individual parameters.

The term "cutting speed" applies to the rate of motion of the cutting tool as it traverses the surface of the workpiece. This parameter's typical unit of measurement is meters

per minute (m/min). Employing a moderate to high cutting speed when machining GG25 gray cast iron is generally advised. Elevating the cutting velocity has the potential to enhance machinability through the reduction of the duration of contact between the tool and workpiece, thus minimizing cutting forces. Nevertheless, exceedingly high cutting speeds may result in thermal problems, such as the production of heat and the likelihood of harm to the workpiece. Determining the ideal cutting speed that achieves a harmonious equilibrium between tool longevity and productivity is of paramount significance.

The term "feed rate" pertains to the pace at which the cutting tool progresses into the workpiece with every revolution. Milling operations typically employ units of measurement such as millimeters per tooth (mm/tooth) or millimeters per minute (mm/min). A moderate feed rate is typically utilized when machining GG25 gray cast iron. Insufficient material removal, heightened tool rubbing, and escalated tool wear are potential consequences of a low feed rate. Conversely, an elevated feed rate may result in amplified cutting forces, probable tool fracture, and diminished surface finish excellence. Selecting a suitable feed rate is of utmost importance as it guarantees the effective removal of chips, maximizes the tool’s lifespan, and results in a desirable surface finish.

The term "depth of cut" pertains to the extent of axial penetration of the tool into the workpiece during the cutting process. Typically, it is quantified in either inches or millimeters. A limited cutting depth is typically favored when working with GG25 gray cast iron. Reducing the depths of the cut too shallow levels can lead to a reduction in cutting forces, a minimization of tool deflection, and an improvement in surface finish. Utilizing depths of cut that surpass the recommended limit may result in amplified cutting forces, heightened heat generation, and diminished tool longevity. When selecting the suitable depth of cut for a given machining process, it is crucial to take into account the rigidity of the machine, the stability of the tool, and the material removal demands.

CHAPTER 5

5. CONCLUSIONS AND RECOMMENDATIONS

5.1. CONCLUSION

This study aimed to determine the optimum cutting parameters during the machining of GG25 gray cast iron using coated carbide insert. The cutting parameters were selected as cutting speed (V_c), feed rate (f), and depth of cut (a_p), while output parameters were chosen as surface roughness, cutting force, and power consumption.

In summary, the study on the machinability of GG25 gray cast iron provides interesting and novel perspectives on the relevant area of research. The findings of this research provide valuable insights for optimizing machining processes and selecting appropriate tooling strategies for components made of GG25 gray cast iron. The aforementioned contributions hold practical significance as they result in better efficiency, cost-effectiveness, and quality in machining operations across different areas.

- The analysis of variance shows that the feed rate has an 82.37% effect on the surface roughness value. The surface roughness value is modeled in this study with 96.58% accuracy. The surface roughness values increased together with the quantity of feed rate. The depth of cut also affects surface roughness by 11.15%. Additionally, there is very little impact of cutting speed on surface roughness. Surface roughness has an error contribution of 3.42%. This indicates that the experiment's surface roughness result was accurate.

- The depth of cut, which contributes 68.82% to the cutting force, is the most important factor. The feed rate's 18.68% contribution gives the impression to show that it was considerable. The modeling accuracy for the cutting force is 97.65%. The cutting force increased in proportion to the feed rate and cut depth. Cutting speed and all other interactions and outcomes are insignificant factors that barely affect cutting force.

- The findings show that the depth of cut and feed rate contribute to 49.34% and 27.24% of power consumption, respectively. Cutting speed is also an important factor in power consumption by a 12.34% contribution. The accuracy of the power consumption was modeled by 91.78%. Similar to the cutting force, the power consumption value likewise increases with the increase in depth of cut and feed rate values.

- Power consumption and cutting force give similar results. The significant factor that affects these two is the depth of cut. The output values also increase with the increase in feed rate and spindle speed. The greater the amount of load required to cut the material, the greater the cutting force. Surface roughness, cutting speed, and power consumption are all positively correlated. As feed rate and cutting depth increase, so does surface roughness. Low feed rates and lower depth of cut may be preferred to create these conditions and also save power consumption. For good surface quality and minimum cutting force and power consumption, a cutting speed of 300, feed rate of 2000, and depth of cut 0.1 are recommended. Spindle speed can be increased to get better surface roughness results. However, with the increase in spindle speed, power consumption and cutting force values are expected to increase.

5.2. Recommendations

This thesis aims to optimize a design's cutting parameters using the Taguchi approach. The study investigated the impact of three distinct cutting parameters, namely cutting speed, feed rate, and depth of cut, on surface roughness (R_a), cutting force (N), and power consumption (W) through the application of analysis of variance (ANOVA). Consequently, a rise in feed rate will lead to a decline in surface quality, while an increase in cutting speed will result in an improvement. The impact of the depth of cut on cutting force and power consumption is noteworthy.

It is advisable to initiate our discourse by delineating the principal pre-established objective of the experiment. The objective of the experiment is to achieve a direct correlation between three cutting parameters and the trend in surface roughness while also ensuring regulated machinability and deliverables. The study's findings suggest that the initial set of cutting parameters did not meet the intended value. It is recommended that a series of tests be conducted to identify potential issues and assess the impact of these parameters on the CNC Milling Center cutting process. The CNC Milling Center is anticipated to possess a recent manufacturing date, exceptional durability, and be outfitted with novel cutting tools, specifically inserts. Furthermore, the present study has thoroughly considered diverse environmental effects and disturbances, including intense vibrations, temperature fluctuations, oxidation, and so forth. Despite the presence of ambient sounds and distractions during the trial, the final results obtained would not have any impact on the overall conclusions of the studies.

The utilization of the Taguchi technique can assist in the analysis of a provided data set by enabling the evaluation of outcomes via the identification of optimal values for significant components and their corresponding response variables. Efficient execution of the cutting procedure is paramount in this experiment, as it is imperative to adhere to the meticulous design criteria. It is essential to optimize the effort and cost involved by accurately determining the appropriate values for surface roughness, cutting speed (V_c), feed rate (f), and depth of cut (a_p) to establish significant correlations. This will enable us to enhance the cutting setups of the CNC milling

center significantly. The selection of our dataset primarily showcases its compatibility for comparative analysis with existing literature, thereby ensuring that the provided cutting parameters can effectively facilitate connectivity with CNC machining and measurement processes.

In order to improve our understanding of the machinability characteristics of GG25 gray cast iron, future investigations should prioritize exploring multi-objective optimization techniques. This study aims to identify the optimal combinations of cutting speed, feed rate, and cutting depth that can effectively minimize surface roughness, cutting force, and energy consumption concurrently. Making use of advanced optimization techniques, such as genetic algorithms or response surface methodology, may improve the discovery of Pareto-optimal solutions that effectively achieve a balance between competing objectives. The proposed methodology aims to provide manufacturers with a range of optimal parameter combinations to choose from, considering their specific priorities and constraints.

In order to improve our understanding of the impact of cutting parameters on surface roughness, cutting force, and power consumption, it is advisable to incorporate a statistical analysis of variance (ANOVA) in the proposed investigations. The application of ANOVA enables the assessment of the statistical significance of individual cutting parameters, as well as their interactions, with respect to performance indicators. Researchers can identify the key factors that influence machinability by conducting statistical significance analysis and allocate their optimization endeavors accordingly.

In order to further improve the machinability of GG25 gray cast iron, it is essential to thoroughly examine the impacts associated with various tool coatings and materials. Further investigation is required to assess the effectiveness of various tool coatings and materials in relation to surface roughness, cutting force, and power consumption. Examining different tool coatings and materials across a range of cutting parameter combinations has the potential to yield substantial findings in identifying optimal tools for enhancing machinability.

The focus of the current investigation was directed toward GG25 gray cast iron. Nevertheless, it is advisable to broaden the scope of the inquiry to encompass additional categorizations of gray cast iron or alternative materials. By conducting an examination of the machinability characteristics of different types of workpiece materials, scholars can broaden the scope of their research and offer a comparative assessment of the effectiveness of machinability. This study aims to support manufacturers in making informed decisions regarding the selection of suitable materials for specific applications, taking into account both machinability and material properties.

Investigating the thermal profile during the machining operation presents interesting possibilities for future research efforts. The impact of temperature on machined surfaces and tool wear is of the utmost significance. Using temperature measurement and analysis techniques during the machining process, researchers aim to expand their understanding of the thermal effects on surface roughness, cutting force, and power consumption. The gathering of this knowledge displays the potential to contribute to the development of temperature control and enhanced methodologies, thereby improving the feasibility of machining procedures.

The research on the expansion of real-time monitoring and control systems in machining processes is currently gaining momentum. The research above endeavors requires an exploration of the integration of sensors and feedback control mechanisms to dynamically regulate cutting parameters based on the determined surface roughness, cutting force, and power consumption. The potential benefits of incorporating real-time monitoring and control into machining operations include the development of adaptive strategies that optimize the machining process by promptly responding to varying circumstances. This approach has the potential to guarantee a uniform and improved level of performance in terms of machinability.

The implementation of the previously mentioned recommendations for future work might help researchers to improve their understanding of the machinability of GG25 gray cast iron and providing practical guidance to improve machining operations in industrial settings.

5.3. FUTURE WORK

The present study delved into the machinability of cast gray iron and explored potential processing scenarios for future research endeavors in this field. Initially, this will make a valuable contribution to future research endeavors aimed at determining the extent to which each machined component will undergo processing in a manner consistent with that of the CNC machine. It is recommended to perform controls before and after the process. Furthermore, this master's thesis suggests that examining theoretical and experimental scenarios will yield valuable insights for future CAM procedures.

The Ballbar tests, in particular, have been analyzed both pre- and post-bench and will provide insight into analogous research in the field. Due to the challenges encountered in investigating the impact of various factors on surface roughness, a mean value was deemed efficacious for numerous participants. The utilization of GG25 gray cast iron, a widely adopted material within the industry, is believed to establish a connection between the industrial and academic sectors. The integration of computer-aided analysis, theoretical analysis, and experimental analysis through ANSYS is believed to yield diverse observations for processing in academic studies of the GG25 CNC Milling Center. There is a belief that there will be increased academic research on GG25 cast iron.

Furthermore, several unforeseen errors were encountered, including those about temperature consistency, environmental factors, human factors, and so forth. Given that our aim was to evaluate their effects, it can be inferred that none of them had a significant impact on it.

REFERENCES

[1] Tasliçukur, Z., Altug, G. S., Polat, S., Atapek, S. H., & Türedi, H. (2012, May). Characterization of microstructure and fracture behavior of GG20 and GG25 cast iron materials used in valves. In *Proceedings of the 21st International Conference on Metallurgy and Materials, Brno, Czech Republic* (pp. 23-25).

[2] Rundman, K. B., & Iacoviello, F. (2001). Cast irons. *Encyclopedia of Materials: Science and Technology, 2nd ed.; Elsevier: Oxford, UK*, 1003-1010.

[3] Martinho, R. P., Silva, F. J., & Baptista, A. P. M. (2008). Cutting forces and wear analysis of Si3N4 diamond coated tools in high speed machining. *Vacuum*, *82*(12), 1415-1420.

[4] Zhou, Y. H. (2017). The application and performance of diamond and PCBN tools in difficult-to-cut materials. In *Solid State Phenomena* (Vol. 263, pp. 90-96). Trans Tech Publications Ltd.

[5] Vopát, T., Kuruc, M., Simna, V., Necpal, M., Buransky, I., Zaujec, R., & Peterka, J. (2018, January). The influence of cutting edge radius size on the tool life of cemented carbide drills. In *Proceedings of the 29th DAAAM International Symposium* (pp. 0421-0425).

[6] Martinho, R. P., Silva, F. J. G., & Baptista, A. P. M. (2007). Wear behaviour of uncoated and diamond coated Si3N4 tools under severe turning conditions. *Wear*, *263*(7-12), 1417-1422.

[7] Fiorini, P. V., Byrne, G., Ahearne, E., & Leopold, J. (2010). Thermo-Mechanical Analysis of High Performance Cutting of Gray Cast Iron.

[8] Saligheh, A., Hajialimohammadi, A., & Abedini, V. (2020). Cutting forces and tool wear investigation for face milling of bimetallic composite parts made of aluminum and cast iron alloys. *International Journal of Engineering*, *33*(6), 1142-1148.

[9] Padmakumar, M., & Dinakaran, D. (2017). Performance evaluation of cryogenically treated and tempered tungsten carbide insert on face milling of gray cast iron. *International Journal of Machining and Machinability of Materials*, *19*(2), 180-191.

[10] Fiorini, P., & Byrne, G. (2016). The influence of built-up layer formation on cutting performance of GG25 gray cast iron. *CIRP Annals*, *65*(1), 93-96.

[11] Dias, L. R. M., & Diniz, A. E. (2013). Effect of the gray cast iron microstructure on milling tool life and cutting force. *Journal of the Brazilian Society of Mechanical Sciences and Engineering*, *35*(1), 17-29.

[12] de Lacalle, L. N. L., Lamikiz, A., Sánchez, J. A., & Arana, J. L. (2002). Improving the surface finish in high speed milling of stamping dies. *Journal of Materials Processing Technology*, *123*(2), 292-302.

[13] Malakizadi, A., Sadik, I., & Nyborg, L. (2013). Wear mechanism of CBN inserts during machining of bimetal aluminum-gray cast iron engine block. *Procedia CIRP*, *8*, 188-193.

[14] Özbeyaz, K. (2014). Prediction of Surface Roughness Value for Machining of Aluminum 1050 Material by Uiıng Artificial Neural Network (Doctoral dissertation, Marmara Universitesi (Turkey)).

[15] Thamizhmanii, S., & Hasan, S. (2006). Analyses of roughness, forces and wear in turning gray cast iron. *Journal of achievements in materials and manufacturing engineering*, *17*(1-2), 401-404.

[16] Souza, J. V. C., Nono, M. C. A., Ribeiro, M. V., Machado, J. P. B., & Silva, O. M. M. (2009). Cutting forces in turning of gray cast iron using silicon nitride based cutting tool. *Materials & Design*, *30*(7), 2715-2720.

[17] Bağcı, E. (2010). *Serbest Formlu Yüzeylere Sahip Parçaların CNC Frezeleme ile İmalatında Tolerans ve Yüzey Pürüzlülük Değerlerinin İyileştirilmesi İçin Kesme Parametreleri ve Stratejilerinin Optimizasyonu* (Doctoral dissertation, Marmara Universitesi (Turkey)).

[18] Karakuş, R. (2020). *Isiya Dayanikli Küresel Grafitli Dökmedemir Malzemelerin İşlenmesinde Kesmeparametrelerinin Yüzey Pürüzlülüğü Veişleme Gürültüsüne Etkileri* (Master Thesis of The Graduate School of Natural and Applıed Sciences of Kirşehir Ahi Evran Universıty, Kirşehir).

[19] Collini, L., Nicoletto, G., & Konečná, R. J. M. S. (2008). Microstructure and mechanical properties of pearlitic gray cast iron. *Materials Science and Engineering: A*, *488*(1-2), 529-539.

[20] Wang, W., Jing, T., Gao, Y., Qiao, G., & Zhao, X. (2007). Properties of a gray cast iron with oriented graphite flakes. *Journal of Materials Processing Technology*, *182*(1-3), 593-597.

[21] Avcı, A., Ilkaya, N., Şimşir, M., & Akdemir, A. (2009). Mechanical and microstructural properties of low-carbon steel-plate-reinforced gray cast iron. *Journal of materials processing technology*, *209*(3), 1410-1416.

[22] Aslantaş, K., Talaş, S., & Taşgetiren, S. (2004). Fracture of a compressor rotor made from gray cast iron. *Engineering Failure Analysis*, *11*(3), 369-373.

[23] Vadiraj, A., Balachandran, G., Kamaraj, M., Gopalakrishna, B., & Rao, K. P. (2010). Studies on mechanical and wear properties of alloyed hypereutectic gray cast irons in the as-cast pearlitic and austempered conditions. *Materials & Design*, *31*(2), 951-955.

[24] Zhao, X., Wang, J. F., & Jing, T. F. (2007). Gray cast iron with directional graphite flakes produced by cylinder covered compression process. *Journal of Iron and Steel Research International*, *14*(5), 52-55.

[25] Choosing the right inserts (2023). CERATIZIT. Accessed from https://cuttingtools.ceratizit.com/us/en/machining-know-how/turning/application-and-technical-info/selection-indexable-inserts.html URL on 30/05/2023.

[26] Moonesan, M., & Madah, F. (2012). Effect of alloying elements on thermal shock resistance of gray cast iron. *Journal of Alloys and Compounds*, *520*, 226-231.

[27] Behnam, M. J., Davami, P., & Varahram, N. (2010). Effect of cooling rate on microstructure and mechanical properties of gray cast iron. *Materials Science and Engineering: A*, *528*(2), 583-588.

[28] Ceratizit (2022). *Selecting the correct indexable inserts*. Ceratizit Cutting Tool. Retrieved February 1, 2023, from https://cuttingtools.ceratizit.com/tr/en/machining-know-how/turning/advisor/selection-indexable-inserts.html

[29] HELLER (2023). *4-axis horizontal machining centres for highly productive machining in all disciplines*. The H series. Retrieved March 29, 2023, from https://uk.heller.biz/products/4-axis-machining-centres-h/?no_cache=1

[30] Akdemir, A., Kuş, R., & Şimşir, M. (2011). Investigation of the tensile properties of continuous steel wire-reinforced gray cast iron composite. *Materials Science and Engineering: A*, *528*(10-11), 3897-3904.

[31] Ipek, R., Selçuk, B., Karamiş, M. B., Kuzucu, V., & Yücel, A. (2000). An evaluation of the possibilities of using borided GG25 cast iron instead of chilled GG25 cast iron (surface properties). *Journal of Materials Processing Technology*, *105*(1-2), 73-79.

[32] Antony, J., & Jiju Antony, F. (2001). Teaching the Taguchi method to industrial engineers. *Work study*, *50*(4), 141-149.

[33] Roy, R. K. (2010). *A primer on the Taguchi method*. Society of Manufacturing Engineers.

[34] Karna, S. K., & Sahai, R. (2012). An overview on Taguchi method. *International journal of engineering and mathematical sciences*, *1*(1), 1-7.

[35] Şahinoğlu, A., & Rafighi, M. (2020). Investigation of vibration, sound intensity, machine current and surface roughness values of AISI 4140 during machining on the lathe. *Arabian Journal for Science and Engineering*, *45*, 765-778.

[36] Korkut, I., & Donertas, M. A. (2007). The influence of feed rate and cutting speed on the cutting forces, surface roughness and tool–chip contact length during face milling. *Materials & design*, *28*(1), 308-312.

[37] Pang, X., Zhang, Y., Wang, C., Chen, Z., Tang, N., & Chen, B. (2020). Effect of cutting parameters on cutting force and surface quality in cutting of articular cartilage. *Procedia CIRP*, *89*, 116-121.

[38] Velchev, S., Kolev, I., Ivanov, K., & Gechevski, S. (2014). Empirical models for specific energy consumption and optimization of cutting parameters for minimizing energy consumption during turning. *Journal of cleaner production*, *80*, 139-149.

[39] Hernández, R. E., Llavé, A. M., & Ahmed, K. (2014). Effects of cutting parameters on cutting forces and surface quality of black spruce cants. *European Journal of Wood and Wood Products*, *72*(1), 107-116.

[40] Polishetty, A., & Littlefair, G. (2021). Advances in conventional machining processes for machinability enhancement of difficult-to-machine materials. In *Advanced Machining and Finishing* (pp. 3-44). Elsevier.

[41] Pawar, S. S., Bera, T. C., & Sangwan, K. S. (2022). Modelling of spindle energy consumption in CNC milling. *Procedia CIRP*, *105*, 192-197.

[42] Bolar, G., Das, A., & Joshi, S. N. (2018). Measurement and analysis of cutting force and product surface quality during end-milling of thin-wall components. *Measurement*, *121*, 190-204.

[43] Aggarwal, A., Singh, H., Kumar, P., & Singh, M. (2008). Optimizing power consumption for CNC turned parts using response surface methodology and Taguchi's technique a comparative analysis. *Journal of materials processing technology*, *200*(1-3), 373-384.